JCI The Journal of Clinical Investigation

IL-34 mediates acute kidney injury and worsens subsequent chronic kidney disease

Jea-Hyun Baek, … , Marco Colonna, Vicki R. Kelley

J Clin Invest. 2015;125(8):3198-3214. https://doi.org/10.1172/JCI81166.

Research Article **Nephrology**

Macrophages (Mø) are integral in ischemia/reperfusion injury–incited (I/R-incited) acute kidney injury (AKI) that leads to fibrosis and chronic kidney disease (CKD). IL-34 and CSF-1 share a receptor (c-FMS), and both cytokines mediate Mø survival and proliferation but also have distinct features. CSF-1 is central to kidney repair and destruction. We tested the hypothesis that IL-34–dependent, Mø-mediated mechanisms promote persistent ischemia-incited AKI that worsens subsequent CKD. In renal I/R, the time-related magnitude of Mø-mediated AKI and subsequent CKD were markedly reduced in IL-34–deficient mice compared with controls. IL-34, c-FMS, and a second IL-34 receptor, protein-tyrosine phosphatase ζ (PTP-ζ) were upregulated in the kidney after I/R. IL-34 was generated by tubular epithelial cells (TECs) and promoted Mø-mediated TEC destruction during AKI that worsened subsequent CKD via 2 distinct mechanisms: enhanced intrarenal Mø proliferation and elevated BM myeloid cell proliferation, which increases circulating monocytes that are drawn into the kidney by chemokines. CSF-1 expression in TECs did not compensate for IL-34 deficiency. In patients, kidney transplants subject to I/R expressed IL-34, c-FMS, and PTP–ζ in TECs during AKI that increased with advancing injury. Moreover, IL-34 expression increased, along with more enduring ischemia in donor kidneys. In conclusion, IL-34-dependent, Mø-mediated, CSF-1 nonredundant mechanisms promote persistent ischemia-incited AKI that worsens subsequent CKD.

IL-34 mediates acute kidney injury and worsens subsequent chronic kidney disease

Jea-Hyun Baek,[1,2] Rui Zeng,[1,2] Julia Weinmann-Menke,[3] M. Todd Valerius,[2,4] Yukihiro Wada,[1,2] Amrendra K. Ajay,[2] Marco Colonna,[5] and Vicki R. Kelley[1,2]

[1]Laboratory of Molecular Autoimmune Disease, [2]Renal Division, Department of Medicine, Brigham and Women's Hospital, Boston, Massachusetts, USA. [3]Department of Nephrology & Rheumatology, Johannes-Gutenberg University Mainz, Mainz, Germany. [4]Harvard Stem Cell Institute, Cambridge, Massachusetts, USA. [5]Department of Pathology and Immunology, Washington University School of Medicine, St. Louis, Missouri, USA.

Macrophages (Mø) are integral in ischemia/reperfusion injury–incited (I/R-incited) acute kidney injury (AKI) that leads to fibrosis and chronic kidney disease (CKD). IL-34 and CSF-1 share a receptor (c-FMS), and both cytokines mediate Mø survival and proliferation but also have distinct features. CSF-1 is central to kidney repair and destruction. We tested the hypothesis that IL-34–dependent, Mø-mediated mechanisms promote persistent ischemia-incited AKI that worsens subsequent CKD. In renal I/R, the time-related magnitude of Mø-mediated AKI and subsequent CKD were markedly reduced in IL-34–deficient mice compared with controls. IL-34, c-FMS, and a second IL-34 receptor, protein-tyrosine phosphatase ζ (PTP-ζ) were upregulated in the kidney after I/R. IL-34 was generated by tubular epithelial cells (TECs) and promoted Mø-mediated TEC destruction during AKI that worsened subsequent CKD via 2 distinct mechanisms: enhanced intrarenal Mø proliferation and elevated BM myeloid cell proliferation, which increases circulating monocytes that are drawn into the kidney by chemokines. CSF-1 expression in TECs did not compensate for IL-34 deficiency. In patients, kidney transplants subject to I/R expressed IL-34, c-FMS, and PTP-ζ in TECs during AKI that increased with advancing injury. Moreover, IL-34 expression increased, along with more enduring ischemia in donor kidneys. In conclusion, IL-34-dependent, Mø-mediated, CSF-1 nonredundant mechanisms promote persistent ischemia-incited AKI that worsens subsequent CKD.

Introduction

Myeloid cells, most notably macrophages (Mø), regulate the inflammatory response to injury. Mø are integral in ischemia/reperfusion injury–incited (I/R-incited) acute kidney injury (AKI) that resolves (1–3) or alternatively leads to chronic kidney disease (CKD) (3). As Mø mediate kidney repair and destruction, we reasoned that the principal molecule required for Mø survival, proliferation, and activation — CSF-1 — is central to regulating the fate of the kidney. Our prior studies show that CSF-1 expression is beneficial in kidneys destined to repair (4) and, conversely, harmful in kidneys destined for autoimmune-mediated chronic disease (3, 5–8).

CSF-1 functions by engaging a high-affinity RTK encoded by the *FMS* proto-oncogene, the CSF-1R (c-FMS, also known as CD115) (9, 10). c-FMS is principally expressed on mononuclear phagocytes, including progenitor cells (11), monoblasts, promonocytes, monocytes (12), Mø, and DCs (13). As *FMS* null mice developed a more severe phenotype than mice lacking CSF-1 (14), this finding led to the discovery of a second c-FMS ligand, IL-34.

IL-34 and CSF-1 have shared and differing properties. Both cytokines promote the growth and survival of monocytes and formation of Mø colonies from BM (15). However, IL-34 is a dimeric glycoprotein without sequence homology to the secreted glycoprotein CSF-1 isoform or any other known cytokine (16). Moreover, IL-34 and CSF-1 differ in spatiotemporal expression in some adult and developing tissues (15), and they have partially overlapping c-FMS binding domains that may be responsible for dissimilar signal-activation kinetics (17). IL-34, but not CSF-1, is critical in the maintenance of tissue-resident homeostatic Mø, such as Langerhans cells and microglia (18). Moreover, while both IL-34 and CSF-1 signal through c-FMS, IL-34 has a second recently uncovered receptor, PTP-ζ, at least in the brain (19). Although CSF-1–mediated mechanisms during renal inflammation are well documented by our laboratory and others (3, 5, 7, 8, 20–25), the role of IL-34 in inflammation, particularly in the kidney, has not been explored. The central issues are: (i) do IL-34–dependent, Mø-mediated mechanisms augment or thwart AKI and subsequent CKD; (ii) are CSF-1 and IL-34 redundant during renal injury; (iii) do IL-34–dependent, Mø-mediated mechanisms within and/or outside the kidney alter renal injury; (iv) are IL-34–dependent mechanisms responsible for shifting the dominant intrarenal Mø phenotype prior to and/or after I/R; and (v) is intrarenal and systemic IL-34 expression relevant to ischemia-incited human AKI and subsequent CKD? Taken together, we tested the hypothesis that IL-34–dependent, Mø-mediated mechanisms promote persistent ischemia-incited AKI and the subsequent CKD.

Authorship note: Jea-Hyun Baek, Rui Zeng, and Julia Weinmann-Menke contributed equally to this work and are co–first authors.
Conflict of interest: V.R. Kelley has an equity interest in Biogen-Idec, a company with research and development interests in lupus.
Submitted: January 26, 2015; **Accepted:** May 14, 2015.
Reference information: *J Clin Invest*. 2015;125(8):3198–3214. doi:10.1172/JCI81166.

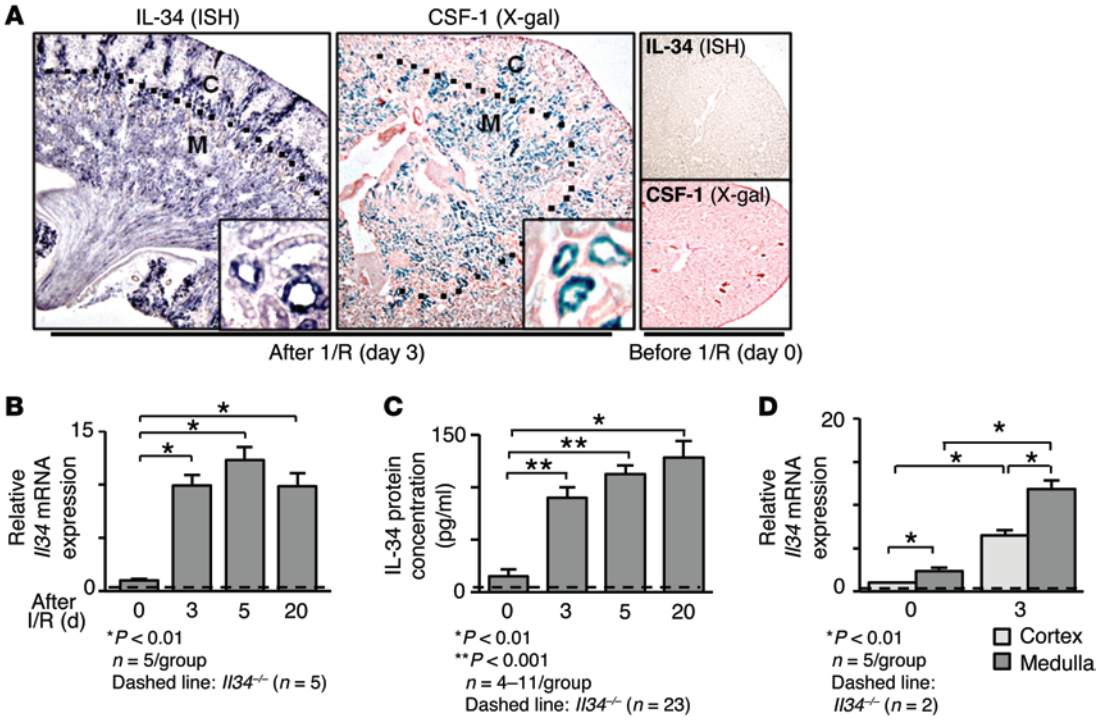

Figure 1. IL-34 is increased in the kidney after I/R. In each figure, expression is analyzed before and after I/R. (**A**) IL-34 expression in B6 TECs identified using in situ hybridization (ISH), and CSF-1 using a CSF-1 reporter mouse (*lacZ* under control of *Csf1* promoter and first intron) stained for β-galactosidase activity (X-gal). Representative photomicrographs (n = 5). Original magnification, ×2.5; inset, ×20. Dotted lines indicate the junction between the cortex (C) and the medulla (M). (**B** and **C**) We detected expression of intrarenal IL-34 transcripts and protein using qPCR (n = 5/group) (**B**) and ELISA (n = 4–11/group) (**C**), respectively. (**D**) *Il34* transcripts in the cortex and medulla were evaluated using qPCR (n = 5/group). *P < 0.01, **P < 0.001. Statistics analyzed using the Mann-Whitney U test. Values are means ± SEM.

Results

Renal ischemic injury incites robust expression of IL-34 and CSF-1 in tubules. Tubules, most notably in the outer medulla, are sensitive to ischemic injury (26). Moreover, the interstitial areas adjacent to ischemic-injured tubules are rich in Mø that often surround and adhere to tubular epithelial cells (TECs) (3). Since IL-34 binds to receptors on Mø and promotes Mø proliferation, we hypothesized that IL-34 is expressed by tubules following ischemic injury. To test this hypothesis, we probed for the locale and magnitude of IL-34 expression in the renal medulla and cortex of B6 mice prior to and after I/R. Using in situ hybridization, we localized ischemia-incited IL-34 expression to tubules (proximal, distal, and collecting ducts) (Figure 1A). We verified this finding using heterozygous IL-34–knockin mice ($Il34^{LacZ/+}$) in which the IL-34 coding region was replaced by the gene coding β-galactosidase (data not shown) (18). By comparison, CSF-1 — evaluated using CSF-1 reporter mice expressing β-galactosidase — and IL-34 are similarly expressed, as both c-FMS ligands are more abundant in the medulla than in the cortex after I/R (Figure 1A). However, while some TECs express both IL-34 and CSF-1 protein (immunostaining), other adjacent TECs express either IL-34 or CSF-1 in inflamed human kidneys (lupus nephritis, data not shown). Moreover, IL-34 transcripts (Figure 1B) and protein (Figure 1C) are robustly expressed after I/R. IL-34 expression rises rapidly during the acute phase (d3, d5) and remains elevated during the chronic phase (d20) (Figure 1, B and C) after I/R. As above, *Il34* transcripts are more pronounced in the medulla than cortex (Figure 1D). By comparison, intrarenal *Il34* transcripts and protein are barely expressed prior to I/R (Figure 1, B and C). $Il34^{-/-}$ kidneys served as negative controls (Figure 1, B and C). Thus, IL-34 and CSF-1 expression is abundant in renal tubules, but not necessarily the same TECs, after I/R.

Overlapping and distinct expression of intrarenal IL-34 receptors after I/R. IL-34 and CSF-1 are ligands for c-FMS, a receptor expressed on Mø and some other hematopoietic and parenchymal cells. However, unlike CSF-1, IL-34 binds to a second functional receptor, PTP-ζ, recently identified in mouse brain. We examined the temporal response of *Fms* and *Ptprz1* after I/R using quantitative PCR (qPCR). Intrarenal *Fms* is expressed in the acute phase (d3, d5) and increases during the chronic phase (d20) after I/R (Figure 2A). We now report the finding that PTP-ζ transcripts (Figure 2B) and protein (Figure 2C) are expressed in the inflamed mouse kidney, albeit less robustly than in brain (data not shown). Moreover, ischemia-induced IL-34 binds to PTP-ζ in the kidney at d20 after I/R (Figure 2D). By comparison, *Fms* is more abundantly expressed than *Ptprz1* during AKI, while both are robustly increased during the chronic phase after I/R (Figure 2, A and B). Using immunostaining, we found PTP-ζ is expressed primarily by TECs and, to a lesser extent, by cells in the inflamed interstitium after I/R (Supplemental Figure 1A; supplemental material available online with this article; doi:10.1172/JCI81166DS1). We verified staining specificity using an isotype control and by titration analysis. To further verify that PTP-ζ is expressed by TECs, we stimulated primary cultured

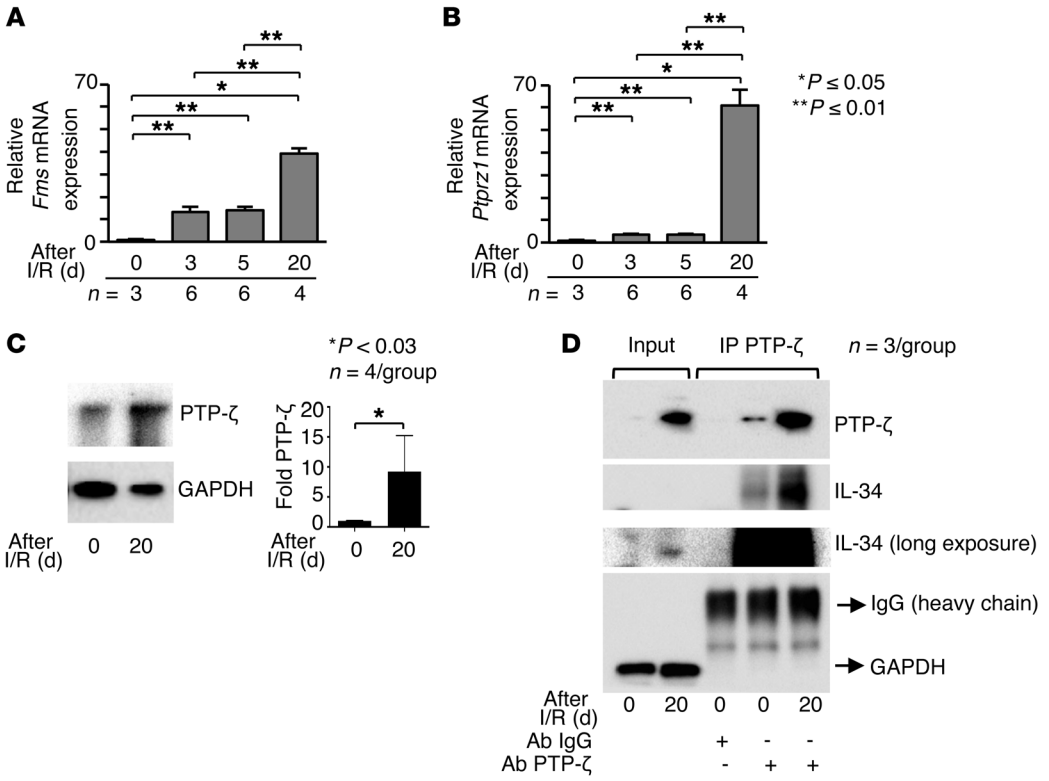

Figure 2. IL-34 receptors have overlapping and distinct expression in the kidney after I/R and IL-34 binds to PTP-ζ. (**A–B**) Intrarenal *Fms* (**A**) and *Ptprz1* (**B**) transcript expression on the same samples using qPCR (repeated 3×). Statistics analyzed using the Mann-Whitney *U* test. $^*P \le 0.05$, $^{**}P \le 0.01$. Values are means ± SEM. (**C**). Intrarenal PTP-ζ protein levels detected by immunoblotting. Quantitation of PTP-ζ relative to GAPDH ($n = 4$). Statistics analyzed using unpaired *t* test (Mann-Whitney *U* test). $^*P < 0.03$. Values are means ± SEM. (**D**) Immunoprecipitation performed from kidney lysates with PTP-ζ or control (mouse IgG) Ab showing IL-34 binding to PTP-ζ ($n = 3$).

TECs with either TNFα or IL-34 and analyzed *Ptprz1* expression using qPCR. *Ptprz1* transcripts are upregulated in response to either stimulus (Supplemental Figure 1B). While Mø ubiquitously expressed c-FMS, it is unlikely that intrarenal Mø express PTP-ζ, as WT BM-derived Mø (BMMø) polarized toward M1 and M2 phenotypes, representing opposite ends of the activation spectrum, do not express PTP-ζ in vitro. (Supplemental Figure 1C). Thus, intrarenal c-FMS and PTP-ζ have overlapping and distinct expression after I/R.

IL-34 mediates loss of tubules evident by the chronic phase after I/R. To determine if IL-34 is central to promoting renal disease, we compared pathology in *Il34*$^{-/-}$ and WT mice in AKI and subsequent CKD after I/R (Figure 3A). Kidney weight and size is more dramatically decreased in WT mice compared with *Il34*$^{-/-}$ mice at d20 and d37 after I/R (Figure 3B). As escalating inflammation drives renal injury, we hypothesized that ischemia-incited renal tubule IL-34 expression promotes leukocyte accumulation in the interstitium, leading to tubule destruction. We detected more tubular pathology (atrophy) and leukocytes in the interstitium in WT compared with *Il34*$^{-/-}$ mice after I/R (Figure 3C). To more fully compare the loss of tubules in *Il34*$^{-/-}$ and WT mice after I/R, we used lotus tetragonolobus lectin (LTL) to detect proximal tubules and dolichos biflorus agglutinin (DBA) to detect collecting ducts. By the chronic phase after I/R, there are far fewer LTL$^+$ and DBA$^+$ cells in WT compared with *Il34*$^{-/-}$ kidneys (d37, Figure 3D). Similar findings appeared at d20 (data not shown). Thus, ischemia-incited IL-34–dependent mechanisms mediate loss of tubules evident during the chronic phase after I/R.

IL-34 mediates tubular injury during AKI. To determine if intrarenal IL-34 fosters acute tubule injury leading to the chronic loss of tubules, we compared the expression of kidney injury molecule 1 (KIM-1) in WT and *Il34*$^{-/-}$ mice after I/R. KIM-1 protein (Figure 4A) and transcripts (data not shown) are more robustly expressed in WT compared with *Il34*$^{-/-}$ TECs during the acute phase after I/R. This suggests that IL-34 expression is central to the initiation of tubule injury. Consistent with IL-34 driving AKI that is reflected in subsequent CKD, serum levels of neutrophil gelatinase–associated lipocalin (NGAL), a reliable marker of AKI progressing to CKD (27) (Figure 4B), and albuminuria (Figure 4C) are higher in WT compared with *Il34*$^{-/-}$ mice at d3 and d20 after I/R. Moreover, we detected more renal fibrosis in WT compared with *Il34*$^{-/-}$ mice during the chronic phase after I/R. Collagen protein was detected using Picrosirius red staining (Figure 4D), and collagen 1 transcripts were detected using qPCR (data not shown). Thus, ischemia-incited IL-34 mediates leukocyte-rich inflammation and tubule injury during AKI and subsequent worsening of CKD.

IL-34 promotes intrarenal myeloid cell accumulation after renal ischemic injury. Because myeloid cells, and in particular Mø, are integral to renal ischemic injury and repair (3), we hypothesized that IL-34 promotes myeloid-mediated renal injury. As anticipated, the accumulation of intrarenal neutrophils (Ly6G$^+$) precedes Mø (F4/80$^+$), and declines rapidly as Mø ascend and remain prominent in WT mice after I/R (Figure 5A). We detected more intrarenal neutrophils and Mø in WT compared with *Il34*$^{-/-}$ during the acute and chronic phase after I/R (Figure 5A). Consistent with the enhanced magnitude of IL-34 expression, neutrophil and Mø accumulation was more abundant in the medulla than cortex (Figure 5A). To identify the intrarenal leukocyte populations in ischemia-incited renal injury, we used flow cytometry (Figure 5B). We verified that fewer intrarenal myeloid cells (CD45$^+$CD11b$^+$) are in *Il34*$^{-/-}$ compared with WT

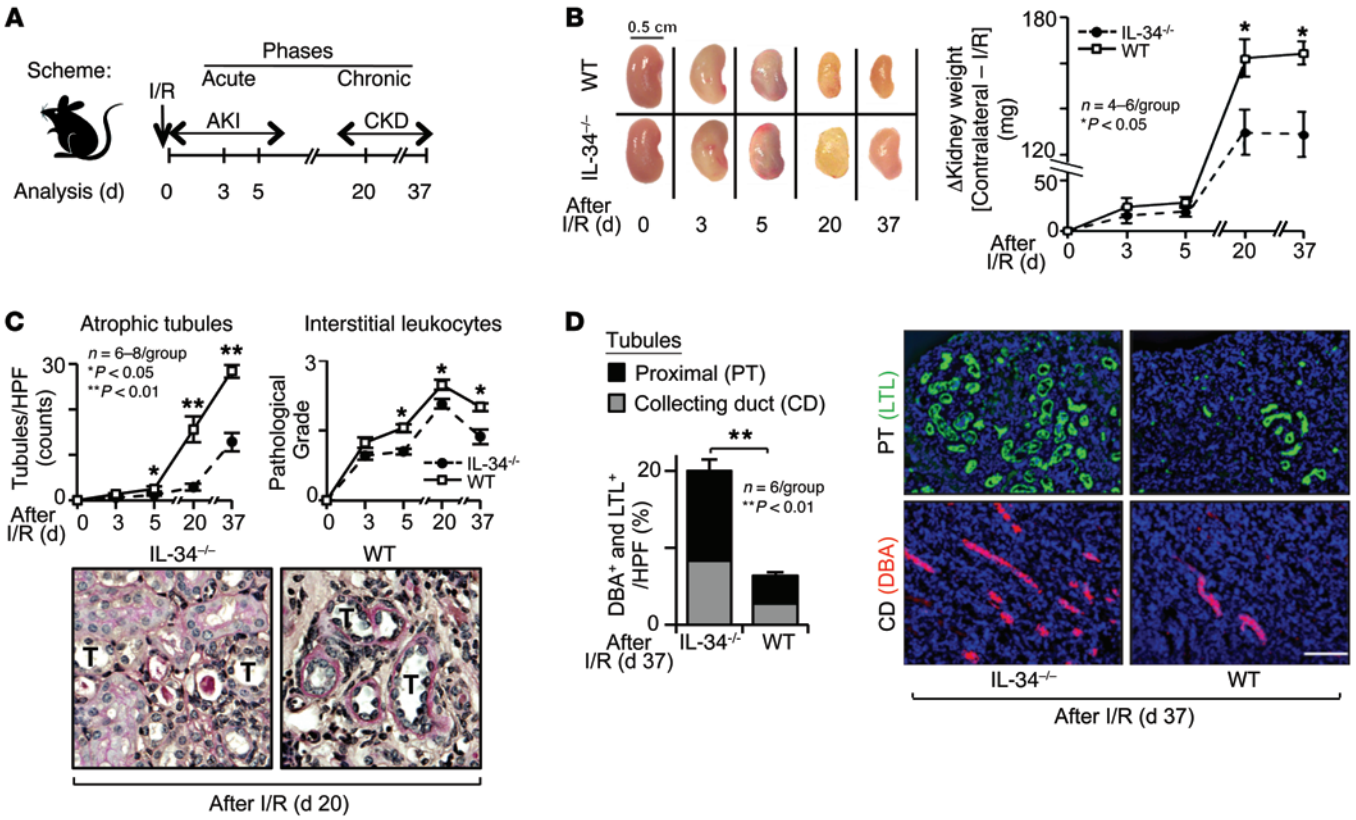

Figure 3. Tubular atrophy and interstitial infiltration are diminished in *Il34*$^{-/-}$ after I/R. (**A**) Scheme: Time-related comparison for AKI and CKD after I/R. (**B**) Representative kidneys from *Il34*$^{-/-}$ and WT B6 mice (left panel) and change in kidney weights (contralateral minus I/R kidney; right panel) after I/R (n = 4–6/group). (**C**) Graphs indicate tubular atrophy and interstitial infiltration grades after I/R injury. Representative photomicrographs after I/R. Original magnification, ×40. T, Tubule (n = 6–8/group). (**D**) LTL identifies proximal tubules, and DBA identifies collecting ducts after I/R. Graphs and representative photomicrographs after I/R. Original magnification, ×10 (n = 6/group). Statistics analyzed using the Mann-Whitney U test. $^{*}P < 0.05$, $^{**}P < 0.01$. Values are means ± SEM.

mice after I/R (Figure 5C). The decline in intrarenal myeloid cells in *Il34*$^{-/-}$ mice is initially due to a reduction in neutrophils (CD45^{+}Ly6G^{+}CD11b^{+}) (Figure 5D) and later results from fewer Mø (CD45^{+}CD11b^{+}Ly6G^{-}F4/80^{+}) (Figure 5E). Thus, ischemia-incited IL-34 expression mediates neutrophil and Mø accumulation in inflamed kidneys.

Renal ischemia incites IL-34 expression that promotes intrarenal Mø proliferation. Mø, but not neutrophils, express the CSF-1 and IL-34 receptor (c-FMS). Thus, signaling through c-FMS on Mø may be responsible for intrarenal Mø accumulation after I/R. We tested the hypothesis that ischemia-incited IL-34 expression in TEC promotes intrarenal Mø proliferation. To test this hypothesis, we used 2 complementary in vivo proliferation assays: in situ immunostaining (Ki67) and flow cytometry (5′-Bromo-2-deoxyuridine [BrdU]). We detected more intrarenal proliferating Mø (Ki67^{+}F4/80^{+} cells) in WT compared with *Il34*$^{-/-}$ mice during the acute phase (d3, d5) and chronic phase (d20) after I/R (Figure 6A). Similarly, intrarenal BrdU^{+} myeloid cells (CD45^{+}CD11b^{+}), and more specifically Mø (CD45^{+}CD11b^{+}Ly6G^{-}), are far more abundant in WT compared with *Il34*$^{-/-}$ mice during the acute and chronic phases after I/R (Figure 6B). The frequency of BrdU^{+} neutrophils remained low throughout the experiment (data not shown). Thus, ischemia-incited IL-34 expression drives intrarenal Mø proliferation.

To determine if IL-34 generated from ischemic TECs directly fosters Mø proliferation, we used several in vitro approaches. We compared Mø (WT BMMø) proliferation after stimulation with supernatant from primary cultured hypoxic *Il34*$^{-/-}$ and WT TECs (Figure 7A). We detected greater Mø proliferation after stimulation with hypoxic WT compared with *Il34*$^{-/-}$ TEC supernatants, as assessed by the MTT assay (Figure 7B). Therefore, hypoxia-incited IL-34 expression by TECs enhances Mø proliferation. Mø stimulated with media alone or containing 20% L929 supernatant plus 10% FCS served as negative and positive controls, respectively. Note, we did not detect a difference in viability of hypoxic WT and *Il34*$^{-/-}$ TECs or normoxic WT and *Il34*$^{-/-}$ TECs, using trypan blue exclusion and propidium iodide (PI) staining (Supplemental Figure 2A). Thus, Mø-stimulating supernatants are generated from equivalent numbers of TECs. As the MTT assay is an index of both proliferation and viability, to verify our proliferation findings, we repeated the above experiment using BrdU incorporation in place of MTT. Similarly, the number of BrdU^{+} Mø rises after stimulation with hypoxic compared with normoxic WT TEC supernatant (Supplemental Figure 2B). Moreover, decreasing the concentration of hypoxic supernatant reduces the magnitude of BrdU^{+} Mø (Supplemental Figure 2B). We verified that IL-34 in TEC supernatant enhances Mø proliferation by adding recombinant IL-34 (rIL-34) to the stimulating hypoxic *Il34*$^{-/-}$ TEC supernatant. Adding increasing

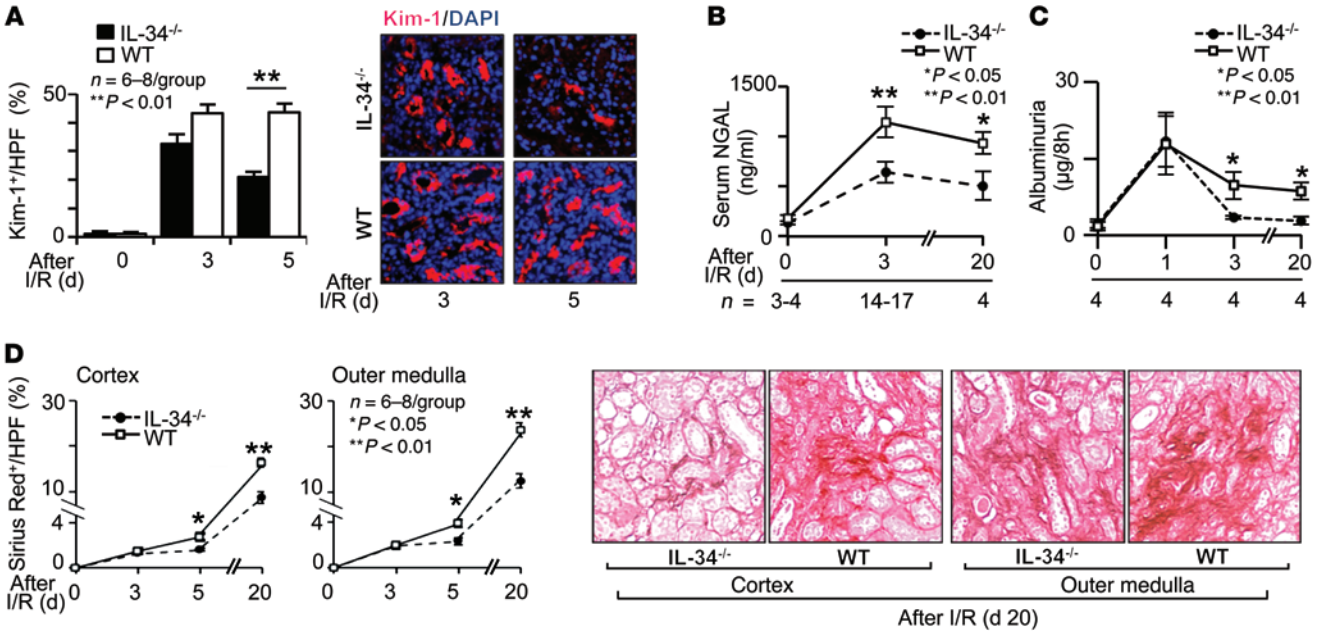

Figure 4. KIM-1 expression and intrarenal fibrosis are decreased in *Il34*$^{-/-}$ after I/R. (**A**) KIM-1 expression (red) immunofluorescence after I/R. Graphs (KIM-1/HPF) and representative photomicrographs. Nuclei are stained with DAPI (blue). Original magnification, ×20 (n = 6–8/group). (**B**) Serum NGAL levels evaluated by Luminex technology. (**C**) Urine albumin excretion over 8 hours evaluated by SDS-PAGE after I/R (n = 3–17/group). (**D**) Renal fibrosis using collagen staining (Picrosirius red). Graphs (% Picrosirius red) and representative photomicrographs after I/R. Original magnification, ×10 (n = 6–8/group). Statistics analyzed using the Mann-Whitney U test. $^{*}P < 0.05$, $^{**}P < 0.01$. Values are means ± SEM.

concentrations of rIL-34 restores Mø proliferation, in a step-wise manner, to WT levels and beyond (MTT assay, Figure 7C). Thus, IL-34 released from hypoxic TEC directly induces Mø proliferation.

Are IL-34 and CSF-1 released into the supernatant of hypoxic TECs both responsible for driving Mø proliferation? IL-34 and CSF-1 (protein) are upregulated in the supernatant of hypoxic WT TEC (Figure 7E). Anti–IL-34 (neutralizing) Ab blockade of IL-34 in supernatants from hypoxic WT TECs partially reduces Mø proliferation (Figure 7D). Similarly, substituting anti–CSF-1 Ab in place of anti–IL-34 Ab also partially reduces Mø proliferation. Moreover, Mø proliferation is reduced to baseline (media alone) levels by blocking CSF-1 in *Il34*$^{-/-}$ hypoxic TEC supernatants (Figure 7D) and by blocking CSF-1 together with IL-34 (using increasing concentrations of Abs) in WT hypoxic TEC supernatants (Supplemental Figure 2C). Thus, hypoxic TEC release IL-34 and CSF-1, which additively are responsible for driving Mø proliferation.

Does CSF-1 compensate for the absence of IL-34 in the ischemic kidney? We found that CSF-1 protein does not increase in the supernatant of either hypoxic or TNFα-stimulated *Il34*$^{-/-}$ compared with WT TECs (Figure 7F). We found similar results analyzing CSF-1 protein in TNFα-stimulated TEC homogenates from *Il34*$^{-/-}$ compared with WT mice (data not shown). This is consistent with equivalent expression of *Csf1* transcripts in TNFα-stimulated *Il34*$^{-/-}$ compared with WT TECs (Supplemental Figure 2D). Thus, CSF-1 does not compensate for the absence of IL-34 in ischemic-injured TECs.

IL-34 stimulates BM myeloid cell proliferation and elevates circulating myeloid cells that are recruited to the kidney after I/R. Intrarenal IL-34 proliferation alone may not account for all IL-34–dependent Mø accumulation in the kidney. In this regard, we detected an elevation of circulating IL-34 after I/R (Figure 8A). Moreover, IL-34 contributes to myeloid cell development and thereby may increase circulating monocytes (15). Therefore, we tested the hypothesis that elevated systemic IL-34 increases the number of circulating myeloid cells that are recruited to the kidney. Using flow cytometry (Figure 8B), we detected an increase in myeloid cells (Figure 8C), neutrophils (Ly6G^{+}Ly6C^{int}, Figure 8D), and inflammatory/migratory monocytes (CD45^{+}CD11b^{+}Ly6G^{-}Ly6C^{hi}, Figure 8E) in circulation during the acute phase after I/R. Thus, IL-34 promotes an increase of circulating neutrophils and monocytes during ischemia-incited AKI.

To determine whether systemic IL-34 promotes the rise in circulating myeloid cells, we tested the hypothesis that IL-34 mediates myeloid cell proliferation in the BM that subsequently enters the circulation. To test this hypothesis, we analyzed myeloid cell BrdU incorporation in BM, blood, and kidney before and after I/R (Figure 8F). BrdU^{+} BM myeloid progenitor cells (SSC^{lo}CD45^{+}CD11b^{+}Ly6G^{-}) are increased in WT compared with *Il34*$^{-/-}$ mice during the acute phase after I/R (Figure 8F, BM). Moreover, we detected elevated circulating BrdU^{+} myeloid cells in WT compared with *Il34*$^{-/-}$ BM during the acute phase after I/R (Figure 8F, Circulation, left). The increase in circulating myeloid cells results from a rise in both neutrophils (Figure 8F, Circulation, middle) and monocytes (Figure 8F, Circulation, right) in WT compared with *Il34*$^{-/-}$ mice. Thus, IL-34 promotes BM myeloid progenitor proliferation, leading to a rise of circulating monocytes and neutrophils after I/R.

To explore whether a rise in myeloid cells in the circulation leads to a greater abundance of myeloid cells in the kidney, we adoptively transferred equal numbers of CSF-1 receptor–labeled BM cells (eGFP^{+} BM cells) into *Il34*$^{-/-}$ and WT mice (3 hours prior

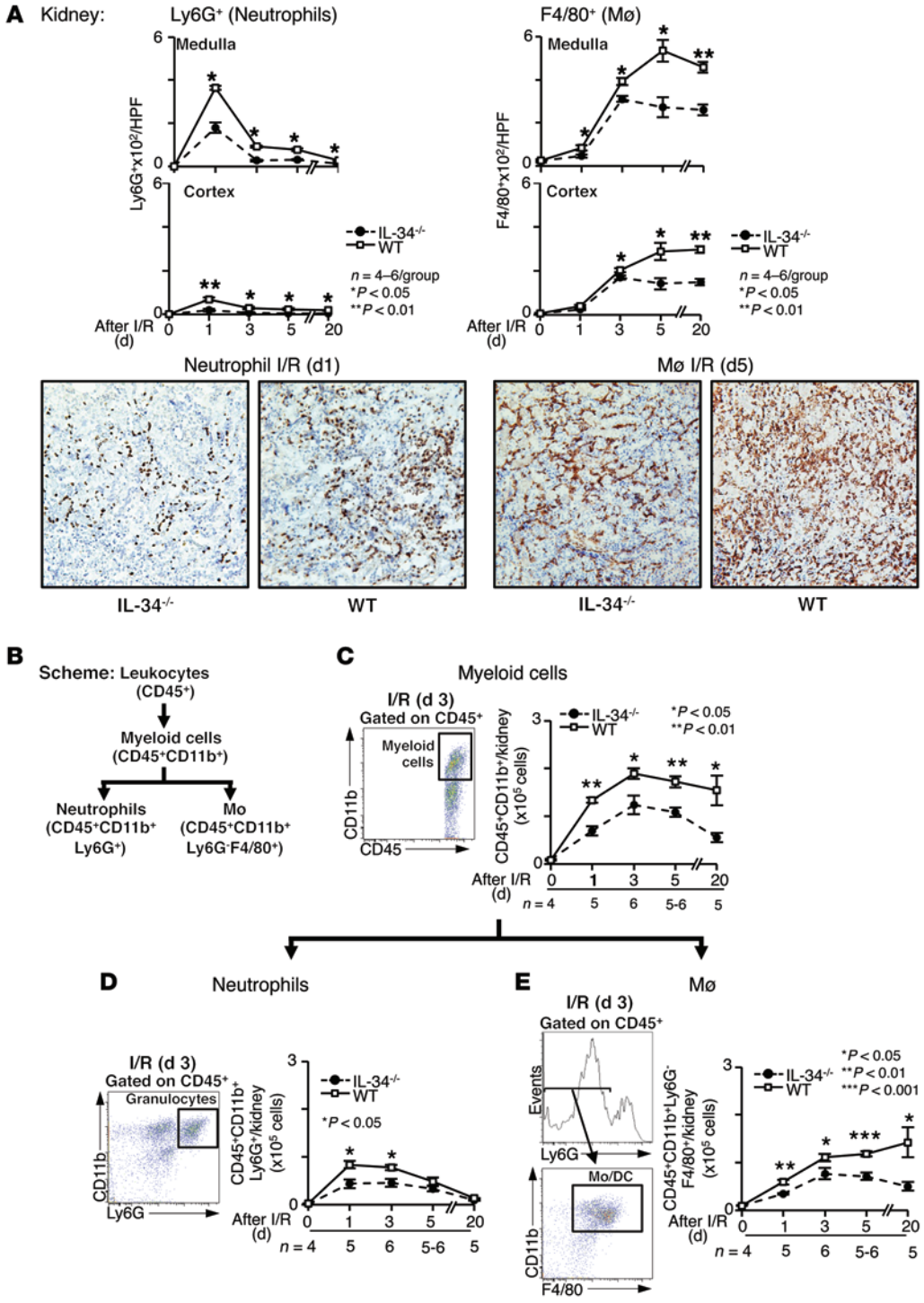

Figure 5. Fewer Mø and neutrophils in *Il34*$^{-/-}$ compared with WT kidneys after I/R. (**A**) Neutrophils (Ly6G$^+$/HPF) and Mø (F4/80$^+$/HPF) in the cortex and medulla identified using immunostaining. Representative photomicrographs. Original magnification, ×10 (n = 4–6/group). (**B**) Scheme depicting cell-sorting approach. (**C**–**E**) Myeloid cell (**C**), neutrophil (**D**), and Mø (**E**) analysis by flow cytometry from the whole kidney (n = 4–6/group). Graphs and representative plots. Statistics analyzed using the Mann-Whitney U test. *P < 0.05, **P < 0.01, ***P < 0.001. Values are means ± SEM.

to sacrifice) after I/R. We found similar eGFP$^+$ BM cells in the circulation, but we found more eGFP$^+$ cells in the kidney in WT than *Il34*$^{-/-}$ mice (Figure 9A). Thus, IL-34 mediates the number of eGFP$^+$ (myeloid cells) recruited to the inflamed kidney. Moreover, we followed the same protocol but injected half the number of eGFP-labeled BM cells into *Il34*$^{-/-}$ mice. We found that the number of labeled cells injected into the circulation is proportional to the number in the kidney (Figure 9A). Thus, increasing myeloid cells in the circulation leads to more myeloid cell trafficking into the inflamed kidney.

IL-34 mediates a rise in intrarenal chemokines that recruit monocytes to the inflamed kidney. Is IL-34 directly or indirectly responsible for enhancing monocyte recruitment to the kidney? To test whether IL-34 directly recruits myeloid cells, we used a transwell system; the upper and lower chambers are separated by a porous membrane (Figure 9B). We determined whether stimulated TECs expressing IL-34 (lower chamber) recruits WT BMMø (upper chamber). To avoid IL-34–mediated Mø proliferation (18- to 22-hour turnover rate) (28), we examined recruitment at 3 hours and 6 hours after BMMø are seeded into the upper chamber. Blocking

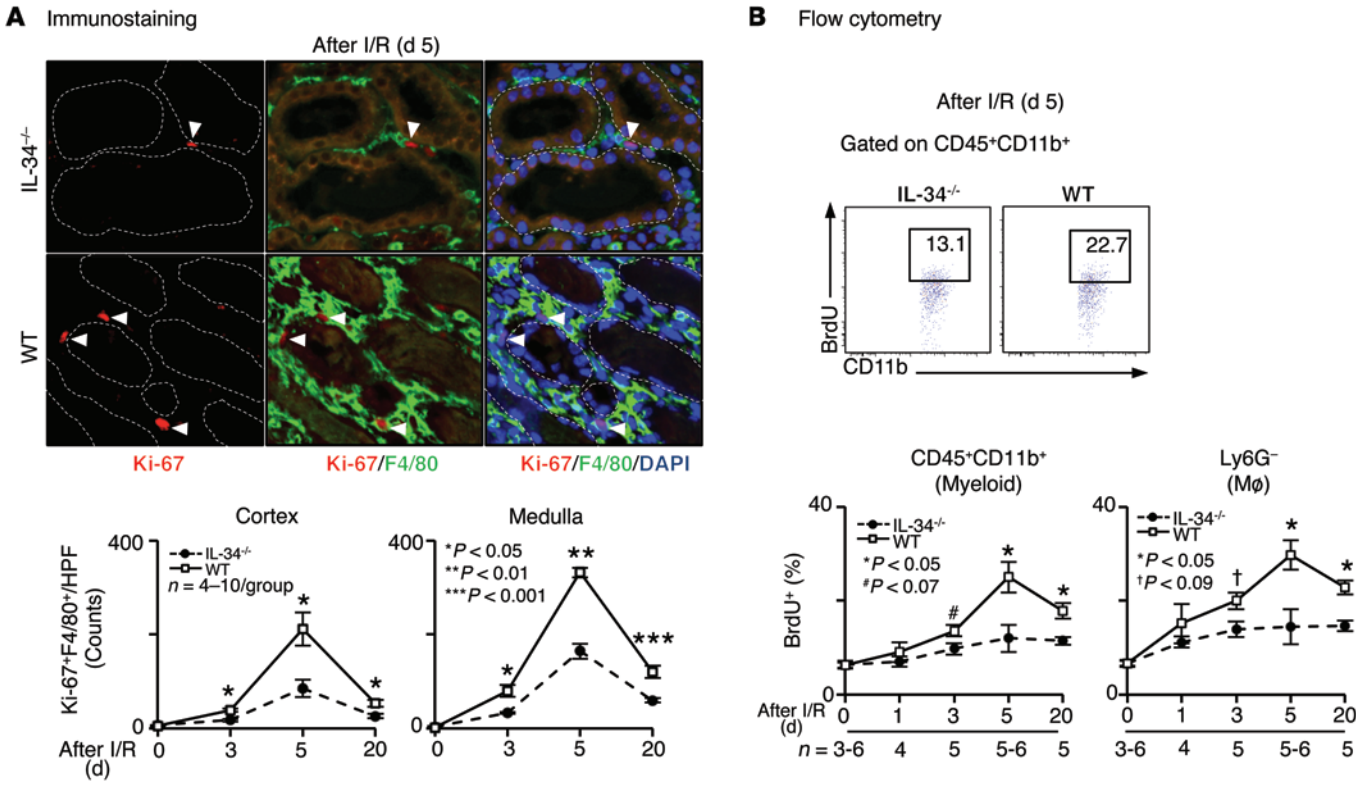

Figure 6. IL-34 expressed by TECs promotes Mø proliferation. In vivo Mø Proliferation: (**A**) Paraffin sections dual-stained with anti-Ki67 (red) and anti-F4/80 (green) Ab to identify proliferating Mø after I/R (n = 4–10/group). Dashed white lines outline tubules, and white arrows indicate Ki67-positive nuclei. Representative photomicrographs and corresponding graphs (Ki67$^+$F4/80$^+$ cells/HPF). Original magnification, ×20. (**B**) Proliferating myeloid cells and Mø are identified by BrdU staining and analyzed using flow cytometry (n = 3–6/group). Statistics analyzed using the Mann-Whitney U test. $^*P < 0.05$, $^{**}P < 0.01$, $^{***}P < 0.001$, $^{\#}P < 0.07$, $^{\dagger}P < 0.09$. Values are means ± SEM.

MCP-1, a well-established Mø chemoattractant, reduced BMMø migration at 6 hours (Figure 9B) and 3 hours (data not shown) after BMMø are seeded into the upper chamber in a dose-responsive manner. In contrast, blocking IL-34 did not alter BMMø migration at 6 hours (Figure 9B) and 3 hours (data not shown) using the same dose range as for MCP-1. This suggests that IL-34 generated by TECs is not directly responsible for Mø recruitment.

We next tested the hypothesis that IL-34 indirectly recruits myeloid cells by increasing intrarenal chemokines. We detected more intrarenal chemokines (MCP-1, also known as CCL2; MIP-1α, also known as CCL3; and CX3CL1, also known as fractalkine), known to recruit Mø, in WT compared with *Il34*$^{-/-}$ after I/R (Figure 10A). The elevation in chemokines is not limited to those recruiting Mø, as intrarenal IP-10, also known as CXCL10, (recruits T cells) is increased and T cells are more abundant in WT compared with *Il34*$^{-/-}$ mice at d5 and d20 after I/R (Figure 10A and Supplemental Figure 3).

To determine whether IL-34 directly stimulates intrarenal chemokine expression, we stimulated TECs with mouse IL-34 in vitro. Stimulating TEC with TNFα (25 ng/ml) readily amplifies chemokine expression (Figure 10B). In contrast, stimulating TECs with varying doses of IL-34 (up to 10 times more than TNFα) does not induce chemokine expression (Figure 10B). This suggests that IL-34 does not directly induce chemokine expression in TECs.

To determine whether chemokines are primarily responsible for recruiting Mø into the inflamed kidney, we blocked G protein–coupled signaling, which blocks chemokine receptors, in BM cells from MacGreen mice (eGFP reporter for c-FMS). For this purpose, we incubated MacGreen BM cells with pertussis toxin (PTx) prior to injecting these cells into WT mice after I/R (d1) (Figure 10C). MacGreen BM cells incubated with heat-inactivated PTx served as a negative control. The viability of MacGreen BM cells treated with PTx or heat-inactivated PTx is 98%–99% (PI staining, data not shown). Blocking G protein–coupled signaling in eGFP$^+$ WT BM cells nearly eliminates all recruitment of these cells into the inflamed kidney (Figure 10C). Taken together, IL-34 mediates the proliferation of BM cells that, in turn, enter the circulation, thereby increasing circulating myeloid cells that are recruited to the inflamed kidney. Moreover, our data suggest that IL-34 indirectly mediates a rise in intrarenal chemokines that recruits myeloid cells into the kidney after I/R. In conclusion, both intrarenal and systemic mechanisms regulate IL-34–dependent accumulation of myeloid cells in the inflamed kidney.

The processes of maintaining kidney-resident Mø and skewing intrarenal-incited Mø phenotypes after ischemia are not dependent on IL-34. Tissue-resident Mø (Ly6C$^-$) are seeded during early development and maintained locally through homeostatic proliferation, independent of monocytes. By comparison, Mø (Ly6C$^+$) derived from monocytes are recruited into inflamed tissues, where they multiply and exert cyto-destructive or cyto-protective functions (28). Recent studies indicate that IL-34 is required to maintain homeostatic cyto-protective tissue-resident Mø (Ly6C$^-$) in some tissues, such as the brain and skin (18, 29). Thus, we determined

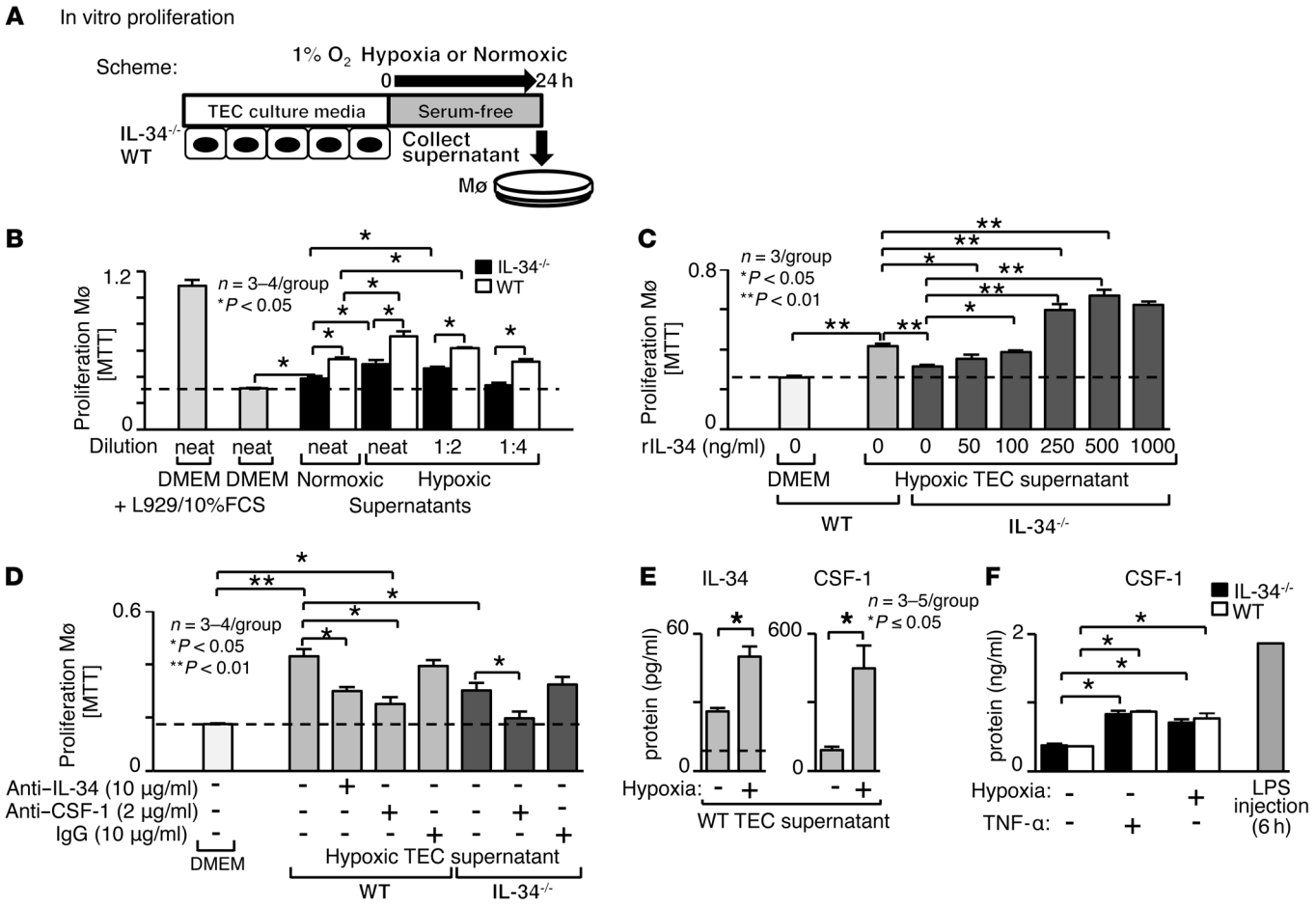

Figure 7. IL-34 generated from hypoxic TECs directly induces Mø proliferation. In vitro Mø proliferation: (**A**) Scheme. (**B**) Cultured WT BMMø stimulated (24 hours) with supernatants of *Il34*$^{-/-}$ and WT TECs after hypoxia or normoxic (24 hours) (MTT assay) (n = 3–4/group). (**C**) To rescue IL-34 in *Il34*$^{-/-}$ TEC supernatant, rIL-34 is added to TEC supernatant prior to stimulating WT BMMø (MTT assay) (n = 3/group). (**D**) To block IL-34 or CSF-1 in WT TEC supernatant, anti–IL-34 or anti–CSF-1 Ab, respectively, are added to the TEC supernatant prior to stimulating WT BMMø (n = 3–4/group). (**E**) IL-34 and CSF-1 protein in supernatant of hypoxic and normoxic (24 hours) TECs evaluated by ELISA (n = 3-5/group). Dotted line represents *Il34*$^{-/-}$ hypoxic supernatant control (n = 2). (**F**) CSF-1 protein in the supernatant of TNFα (25 ng/ml) stimulated and hypoxic *Il34*$^{-/-}$ and WT TECs. CSF-1 control is serum from mice injected i.p. with LPS (25 μg) (n = 3–5/group). Statistics analyzed using the Mann-Whitney U test. $^{*}P \leq 0.05$, $^{**}P < 0.01$. Values are means ± SEM.

whether IL-34 is required for the maintenance of tissue-resident Mø in the kidney. We detected equivalent numbers of Ly6C^{-} Mø (CD45^{+}Ly6C^{-}CD11b^{+}Ly6G^{-}F4/80^{+}) in *Il34*$^{-/-}$ compared with WT kidneys (nonmanipulated) (Supplemental Figure 4C) and in the circulation (Supplemental Figure 4B). Moreover, the absence of IL-34 does not alter kidney development, as *Il34*$^{-/-}$ and WT kidneys are the same size (kidney/body weight, Supplemental Figure 4A) and appear similar by histology (data not shown). Thus, IL-34 is not required for kidney-resident Mø homeostasis. Once in the inflamed kidney, Ly6C^{-} Mø may either reflect an expansion of tissue-resident Mø or invading monocytes that switch from Ly6C^{+} to Ly6C^{-}. We detect equivalent frequencies of Ly6C^{-} and Ly6C^{+} Mø in WT and *Il34*$^{-/-}$ kidneys, and we detect more Ly6C^{+} and Ly6C^{-} Mø in WT compared with *Il34*$^{-/-}$ kidneys after I/R (Supplemental Figure 4). While there are far more Ly6C^{-} than Ly6C^{+} Mø in both WT and *Il34*$^{-/-}$ kidneys, it remains unclear whether this reflects an expansion of tissue-resident or invading monocytes. Taken together, IL-34 expression does not skew Mø toward either Ly6C^{+} or Ly6C^{-} phenotype in the kidney prior to or after I/R.

Broadly, Mø responding to local signals are divided into functional states at opposite ends of the activation spectrum (referred to as M1 and M2). Simplistically, M1 Mø promote injury, while M2 are reparative (30–32). We tested the hypothesis that an IL-34–dependent shift in Mø phenotypes promotes AKI. We found a predominance of M1-like Mø (CD45^{+}Ly6G^{-}F4/80^{+}NOS-2^{+}TNFα^{+}) during the acute phase that shift to the M2 (CD45^{+}Ly6G^{-}F4/80^{+}Arginase-1^{+}Dectin-1^{+}CD206^{+}) phenotype during the chronic phase in WT mice after I/R (Supplemental Figure 5). The predominance of M1-like Mø during the acute phase and M2-like Mø (CD45^{+}Ly6G^{-}F4/80^{+}Arginase-1^{+}Dectin-1^{+}CD206^{+}) during the chronic phase is more pronounced in WT compared with *Il34*$^{-/-}$ mice. However, IL-34 does not skew intrarenal Mø toward either an M1-like or M2-like phenotype, as the frequency of these phenotypes are similar in WT and *Il34*$^{-/-}$ mice after I/R (Supplemental Figure 5). Thus, IL-34 expression does not shift intrarenal Mø phenotypes toward either an M1 or M2 phenotype, but rather expands the accumulation of Mø phenotypes.

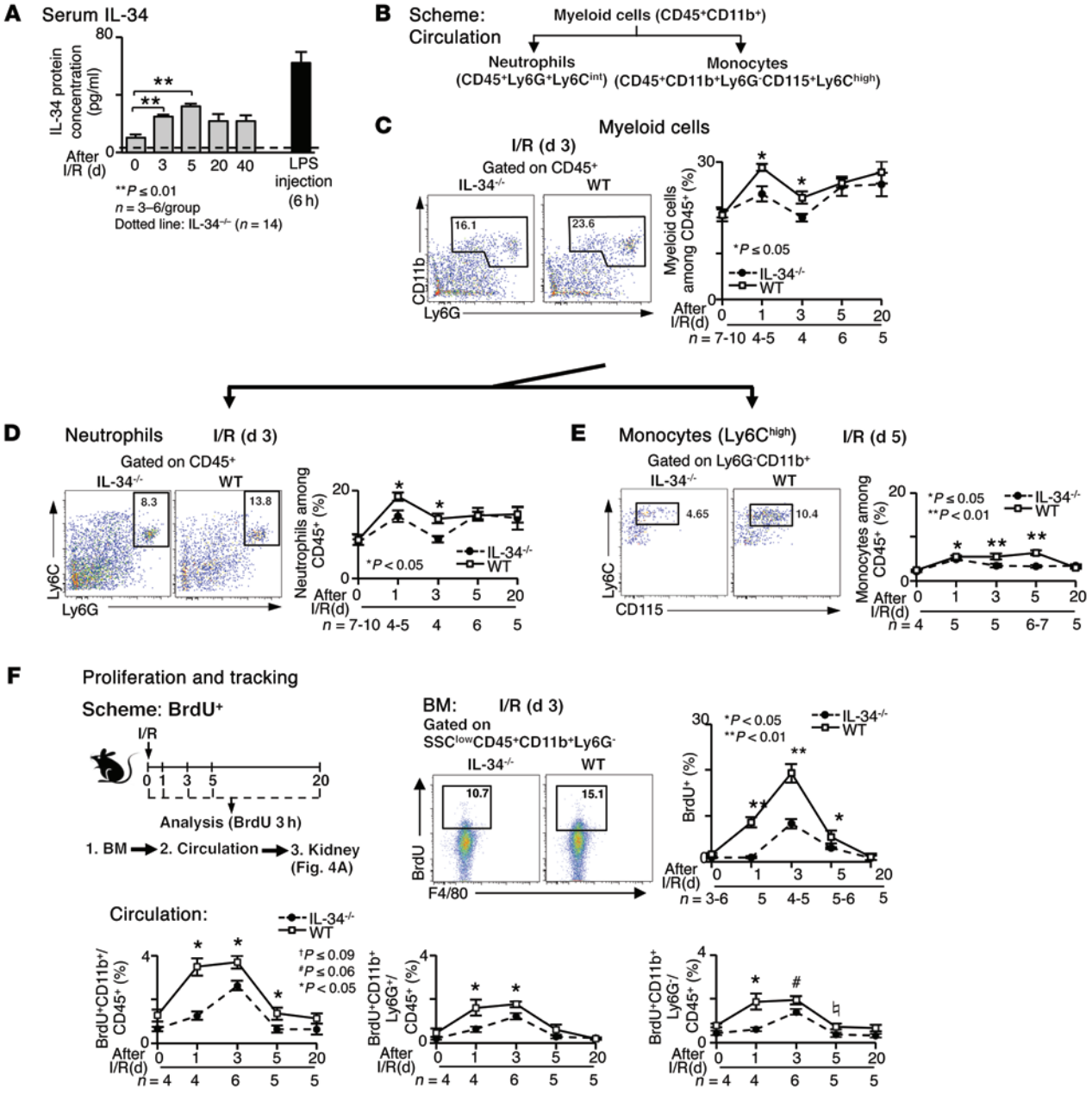

Figure 8. IL-34 promotes myeloid cell proliferation in BM and increases circulating monocyte. (**A**) IL-34 protein in the circulation of WT mice after I/R measured using an ELISA (n = 3–6/group). The serum collected 6 hours after LPS injection (25 μg, i.p.) into WT mice is used as a positive control, and serum from *Il34*$^{-/-}$ mice (dashed line) is used as a negative control (n = 14). (**B**–**E**) Scheme (**B**), graphs, and plots using flow cytometry analysis to evaluate the frequency of myeloid cells (**C**), neutrophils (**D**), and monocytes (**E**) in the circulation after I/R (n = 4–10/group). (**F**) Scheme. BrdU (2 mg) was injected 3 hours prior to sacrifice. Data was analyzed using flow cytometry. BM: Proliferating SSC^{lo} myeloid cells in BM. Circulation: Proliferating circulating myeloid cells, Ly6C^{hi} neutrophils and monocytes mice (n = 3–6/group). Statistics analyzed using Mann-Whitney U test. $^{*}P < 0.05$, $^{**}P < 0.01$, $^{\#}P \leq 0.06$, $^{\dagger}P < 0.09$. Values are means ± SEM.

IL-34 and IL-34 receptors are upregulated in TECs after I/R in human kidneys. IL-34 is upregulated in ischemia-incited human inflamed kidneys. Because I/R injury is an inevitable consequence of the kidney transplant procedure and prolonged ischemia leads to poorer graft survival (33), we probed for IL-34 in the engrafted and rejected kidney during the first 6 months after transplantation (acute phase) (Supplemental Table 1A). IL-34 is upregulated in the engrafted kidney compared with the donor kidney (living and deceased after reperfusion) and rises even higher during acute kidney rejection (Figure 11A). In mice, after I/R, IL-34 is expressed predominately by TECs (Figure 1A), and IL-34 mediates the survival and proliferation of Mø and the accumulation of neutrophils. Therefore, we tested the hypothesis that intrarenal IL-34 expression promotes the accumulation of intrarenal myeloid cells. Consistent with the level of IL-34 expression in TECs, we detected far more Mø (CD68^{+}) and neutrophils (Ly6G^{+}) in

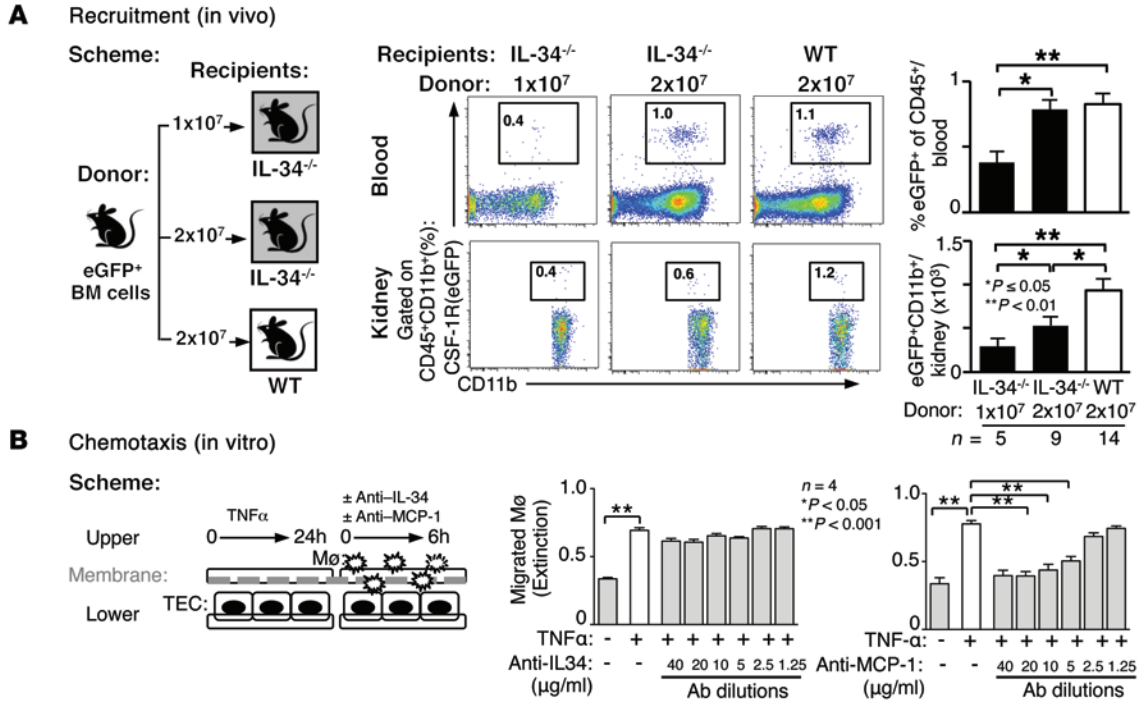

Figure 9. IL-34 recruits BM derived cells to the kidney by indirectly amplifying intrarenal chemokines after I/R. (**A**) *Il34*$^{-/-}$ and WT mice are intravenously injected either with the same or half the number of BM cells from MacGreen mice 3 hours before sacrifice at d1 after I/R. Blood and kidney are collected and analyzed by flow cytometry for the number and frequency of donor cells, respectively (n = 5–14/group). (**B**) Induction of BMMø migration to stimulated TEC supernatants incubated with and without diluted anti–IL-34 and anti–MCP-1 Abs (n = 4/group), repeated 3×. Statistical differences are determined by Mann-Whitney U test. *P < 0.05, **P < 0.01. Values are means ± SEM.

the renal interstitium in engrafted compared with donor kidneys that are even more pronounced during kidney transplant rejection (Supplemental Figure 6). Note, Mø are far more abundant (2 times) than neutrophils in the transplanted kidneys. Thus, ischemic injury in human kidneys upregulates IL-34 in TECs and simultaneously increases renal interstitial Mø and neutrophils. Accompanying IL-34 expression by TECs, we detected a pronounced rise in serum IL-34 during rejection compared with engraftment and healthy controls (Figure 11B). IL-34 serum levels reflected intrarenal IL-34 expression, as serum and TEC-derived IL-34 correlate with the magnitude of IL-34 expression in rejected and engrafted kidney transplants (Figure 11C).

To further explore the relationship of I/R and IL-34 in patients, we compared deceased donor kidney (more ischemic) with living donor kidneys (less ischemic) prior to and after reperfusion (Supplemental Table 1B). IL-34 expression is higher in human deceased and living donor kidneys after reperfusion compared with before reperfusion (Figure 12A). Moreover, IL-34 expression is elevated in deceased compared with living donor kidneys both before and after reperfusion (Figure 12A). This suggests that intrarenal IL-34 expression rises with increasing renal ischemia in patients receiving a kidney transplant.

To determine whether the IL-34 receptors are upregulated along with IL-34, we probed for PTP-ζ and c-FMS expression in the same human kidney transplants (Figure 11A). PTP-ζ and c-FMS expression are both upregulated in kidney transplants (Figure 11A). Moreover, PTP-ζ and c-FMS are expressed by TECs and in some cells in the interstitium (Figure 11A). As PTP-ζ is more abundant in the chronic compared with acute phase after I/R, we compared PTP-ζ in patients with acute and chronic kidney transplant rejection. Similar to our findings in mice, PTP-ζ is more abundant in chronic compared with acute kidney transplant rejection (Figure 12B). Since IL-34 and IL-34–receptor expression in mouse and human kidneys are similarly upregulated within ischemia-incited renal injury, and IL-34 promotes ischemia-incited AKI, we speculate that IL-34 mediates human renal injury.

Discussion

We report here the finding that IL-34 promotes Mø-mediated persistent ischemia-incited AKI, worsening subsequent CKD. IL-34 expression is upregulated in TECs during the acute phase and remains elevated during the chronic phase after I/R, and it is maximal in the medulla, the site most sensitive to I/R injury. By comparison, the receptors for IL-34, c-FMS and PTP-ζ, are maximally expressed in the chronic phase after I/R. Intrarenal IL-34 promotes Mø-mediated TEC destruction during the acute and, subsequently, the chronic phase after ischemic injury. Intrarenal IL-34 fosters Mø accumulation via 2 distinct mechanisms: enhancing Mø proliferation locally in the kidney and releasing IL-34 into the circulation, leading to a rise in BM myeloid cell proliferation that subsequently enter the circulation and increase circulating monocytes. The IL-34–dependent rise in circulating myeloid cells provides a larger pool of myeloid cells available for recruitment to the inflamed kidney. IL-34 does not directly recruit monocytes, but rather increases intrarenal inflammation and thereby chemokines that draw circulating myeloid cells to the inflamed kidney.

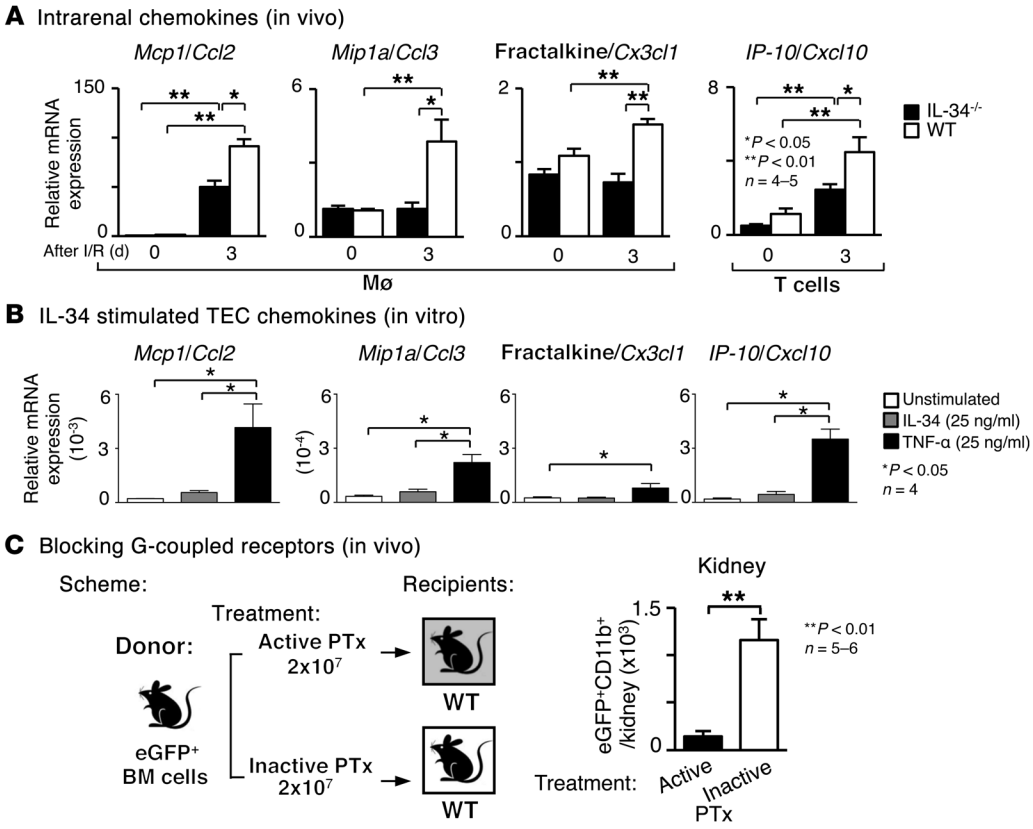

Figure 10. IL-34 mediates a rise in intrarenal chemokines that recruit monocytes to the inflamed kidney. (**A**) Kidneys are analyzed for transcript expression of selected chemokines at d3 after I/R using qPCR (n = 4–5/group). (**B**) TECs after stimulation with IL-34 and TNFα are analyzed for transcript expression of select chemokines (n = 4/group), repeated 2×. (**C**) Recruitment of myeloid cells tested as in **A**. To inhibit G-coupled receptors, donor cells are pretreated with PTx (100 ng/ml, 1 hour). Control: donor cells pretreated with heat-inactivated PTx (n = 5–6/group). Statistical differences are determined by Mann-Whitney U test. $^*P < 0.05$, $^{**}P < 0.01$. Values are means ± SEM.

I/R injury is an inevitable consequence of the kidney transplantation procedure. We detected increased IL-34 expression by TECs in human transplanted kidneys. Moreover, IL-34 is increased in the serum of recipients with transplanted kidneys and rises higher with advancing renal inflammation. CSF-1 does not compensate for the absence of IL-34. Thus, targeting IL-34 is a potential therapeutic to suppress AKI and subsequent CKD. Further detailed studies are required to determine whether targeting IL-34 during the chronic phase after I/R alone suppresses CKD.

While IL-34 and CSF-1 share a common receptor and partially overlap in functions, the list of their distinct actions is rapidly expanding (34-37). The roles of IL-34 and CSF-1 clearly differ during growth and development. For example, *Csf1*$^{op/op}$ mice lacking a functional CSF-1 express an obvious phenotype, including reduced body and kidney size and weight, frailty, defective skeletal and tooth formation, and infertility (24, 38). By comparison, other than the microscopically evident loss of Langerhans cells and microglia (18, 29), *Il34*$^{-/-}$ mice express a normal phenotype, including normal body and kidney size and weight, and similar numbers of circulating and intrarenal monocytes and neutrophils compared with WT mice. The recent discovery of a second IL-34 receptor, PTP-ζ, in neural progenitor and glial cells in the brain may be responsible for some differing functions of IL-34 and CSF-1. Intrarenal PTP-ζ is expressed primarily by TEC and binds to IL-34. Moreover, PTP-ζ is more robustly expressed during the chronic compared with acute phase after ischemia-incited renal injury. By comparison, intrarenal c-FMS expression is more abundant than PTP-ζ during the acute phase, while both IL-34 receptors are maximally expressed during the chronic phase after I/R. PTP-ζ and c-FMS may be central to fibrosis, as these transcripts rise along with the loss of tubules and replacement by fibrosis. Moreover, IL-34 and CSF-1 are overexpressed in chronic hepatitis C liver fibrosis and induce profibrotic Mø (39). Dissecting the role of PTP-ζ in kidney disease may be complex, as this receptor binds to and signals through the actions of multiple ligands (40), including the heparin binding growth factors pleiotrophin and midkine (41), the cell surface protein contactin (42), and the extracellular matrix protein tenascin-R (43). It will be intriguing to pinpoint the PTP-ζ– and/or c-FMS–mediated IL-34–dependent and –independent mechanisms that may be central to intrarenal fibrosis.

IL-34 and CSF-1 are the principle molecules released from TECs that mediate intrarenal Mø proliferation, as eliminating both of these molecules, but not either alone, reduces Mø proliferation to baseline levels. Moreover, CSF-1 does not compensate for the lack of IL-34 during inflammation, as ischemia-incited renal injury is diminished in *Il34*$^{-/-}$ compared with WT mice, and stimulated *Il34*$^{-/-}$ and WT TEC express similar levels of CSF-1. This is consistent with the absence of a compensatory increase in *Il34* mRNA expression in *Csf1*$^{op/op}$ mice in several noninflamed tissues (ear, skeletal muscle, liver, salivary gland, and spleen) (15). Moreover, elevated intrarenal IL-34 is not restricted to I/R injury. IL-34 protein and transcripts are abundantly upregulated in MRL-*Fas*^{lpr} mice with spontaneous CKD (lupus nephritis, unpublished data), and intrarenal *Il34* transcripts are elevated in the kidney of other models with lupus nephritis (44). These findings have seeded studies to clarify whether IL-34 is a potential therapeutic target for chronic kidney diseases with multiple etiologies.

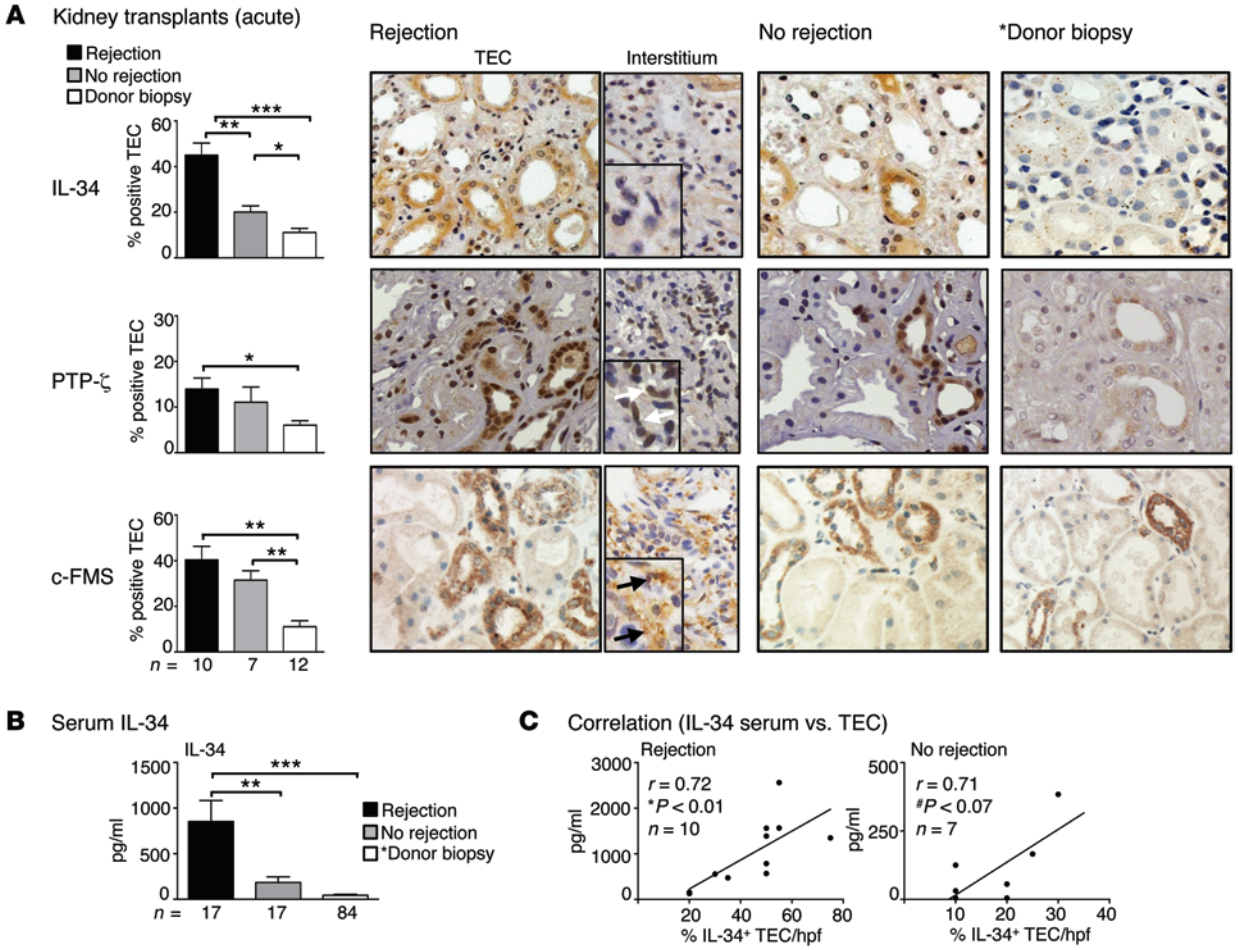

Figure 11. Intrarenal IL-34 is increased in engrafted and rejected kidney transplants. (**A**) Kidney biopsies include: the *donor (defined as donor biopsy from living and deceased donors after reperfusion) and engrafted and rejected (acute cellular) transplant (within 6 months of transplant). IL-34, PTP-ζ, and c-FMS expression detected in renal biopsy by immunostaining (brown reaction product) in TECs and interstitium. White arrows denote PTP-ζ–expressing cells, and black arrows denote c-FMS–expressing cells. Representative photomicrographs. Original magnification, ×40 (n = 7–12/group). (**B**) Serum IL-34 expression in *donor and transplanted kidneys quantified by an ELISA (n = 17–84/group). (**C**) Correlation of serum and IL-34$^+$ TEC expression (n = 7–10/group). Demographic and patient clinical characteristics detailed in Supplemental Table 1. Statistics analyzed by the Mann-Whitney U test. $^*P < 0.05$, $^{**}P < 0.01$, $^{***}P < 0.001$. Values are means ± SEM.

Are the actions of IL-34 and CSF-1 similar or distinct in ischemia-incited renal injury? While ischemia-induced IL-34 drives AKI and thereby worsens subsequent CKD, our prior studies (4) and others (24, 25) indicate that CSF-1 hastens AKI repair after I/R. However, CSF-1 mediates repair in AKI and conversely escalates spontaneous (MRL-*Fas*^{lpr} lupus nephritis) (3, 5, 7, 8, 20) and induced (unilateral ureteral obstruction) (22, 23) CKD. This divergent role of CSF-1 is analogous to epidermal growth-factor receptor signaling in AKI and CKD. (45, 46). One caveat concerning the distinct actions of IL-34 and CSF-1 in AKI relates to comparing differing models/methods (CSF-1–transgenic, CSF-1–injected, and CSF-1–deficient osteopetrotic *Csf1*$^{op/op}$ mice, versus *Il34*$^{-/-}$ mice) and experimental I/R protocols. Nevertheless, our data support the concept that the roles of IL-34 and CSF-1 are dissimilar in renal injury, a finding consistent with nonredundant features of these c-FMS ligands.

Unlike CSF-1, IL-34 does not directly recruit monocytes into the inflamed kidney (7). Our data suggest that intrarenal IL-34 incites inflammation and the expression of chemokines, such as MCP-1, that recruit monocytes into the inflamed kidney (47). This is consistent with markedly weak IL-34–mediated direct migration of the mouse monocyte/Mø cell line (J774A.1) in vitro (17). Moreover, IL-34–dependent elevated intrarenal inflammation is a plausible explanation for the rise in neutrophils in the circulation and kidney in WT compared with *Il34*$^{-/-}$ mice (48). Taken together, IL-34 directly and indirectly mediates AKI, worsening subsequent CKD.

IL-34 fosters homeostatic, protective, tissue-resident Mø in select tissues. Mø are divided according to their origin. Tissue-resident Mø (Ly6C$^-$) are seeded during early development; are maintained locally through homeostatic proliferation, independent of monocytes; patrol peripheral tissues; and exert a broad range of immunoregulatory, cyto-protective functions (28). By comparison, monocyte-derived Mø (Ly6C$^+$) are recruited into inflamed tissues, where they multiply and exert cyto-destructive or cyto-protective functions (28). Initial in vitro evidence suggested that IL-34 promotes the expansion of cyto-protective Mø in tissues, as IL-34–stimulated Mø express an immunosuppressive cytokine

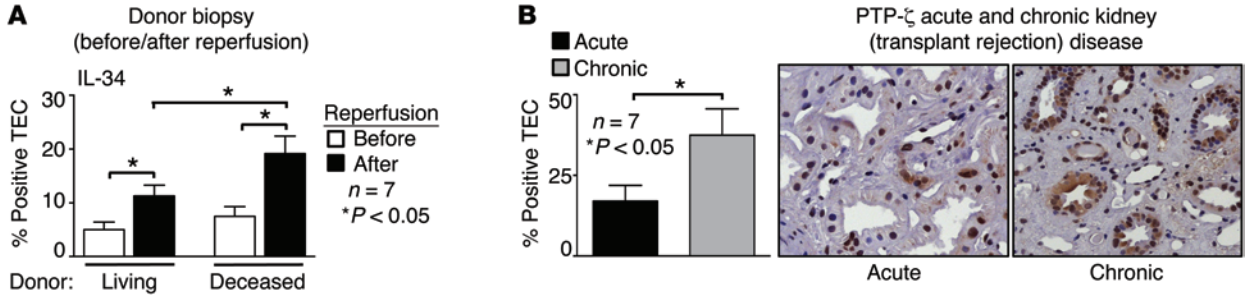

Figure 12. IL-34 is upregulated in reperfused deceased donor kidneys, and PTP-ζ is more abundantly expressed in chronic than acute transplant rejected kidneys. (**A**) IL-34 expression in living and deceased donor biopsies before and after reperfusion (n = 7/group). (**B**) PTP-ζ expression in acute and chronic disease in human kidney transplants (n = 7/group). Graph and representative photomicrographs. Original magnification, ×40. Demographic and patient clinical characteristics detailed in Supplemental Table 1. Statistics analyzed by the Mann-Whitney U test. *P < 0.05. Values are means ± SEM.

profile (IL-10^{hi}, IL-12^{lo}), reduce Mø mediated T cell stimulation and proliferation, and skew human monocytes toward a M2 phenotype (49). Moreover, IL-34 is required for the maintenance of homeostatic cyto-protective tissue-resident Mø (Ly6C$^-$) in brain and skin (18, 29). We now report that IL-34 does not maintain kidney-resident Mø, as the number and frequency of Ly6C$^-$ is similar in nonmanipulated *Il34*$^{-/-}$ and WT kidneys. Thus, IL-34 is not required to maintain homeostatic cyto-protective Mø in the resting kidney.

IL-34 mediates intrarenal Mø accumulation but does not shift phenotypes during AKI and subsequent CKD. Several previous studies indicate that M1-like Mø drive injury and M2-like Mø mediate repair during renal inflammation (1, 3, 25). Our findings are consistent with a rise in IL-34–dependent M1-like Mø mediating more severe AKI. Although the abundance of M2-like Mø in ischemia-incited CKD is seemingly at odds with some prior studies in renal inflammation, there are possible explanations. Growing evidence shows M2-like Mø are the dominant phenotype in fibrotic lesions of CKD of many etiologies. For example, the abundance of M2-like Mø in human and mouse polycystic kidney disease (PKD), contribute to the progression of renal disease by promoting cyst growth and fibrosis (50). Similarly, M2-like Mø proliferation and infiltration is associated with tubular injury and progression of fibrosis during inflammation in human kidney transplant allografts (51, 52). Moreover, insufficient renal epithelial healing in mice promotes an expansion of M2-like Mø that accelerates fibrogenesis (reviewed in ref. 53). These findings in kidney disease are in keeping with the profibrotic functions of M2-like Mø in the liver (54). As we find a predominance of M2-like Mø–expressing markers (CD 206$^+$, Arginase-1$^+$, Dectin-1$^+$) linked to fibrosis (55–57) in fibrotic kidneys after I/R, our findings are consistent with the concept that these intrarenal Mø are profibrotic. Since fibrosis is a protective response to tissue injury, M2-like Mø may mediate both repair and fibrosis. Moreover, when renal injury is severe, as in our study, fibrosis results in substantial loss of tissue and CKD. Thus, it is not inconsistent that some have found intrarenal M2-like Mø during renal repair, while we found M2-like Mø in fibrotic kidneys during CKD. To add to the complexity of defining the roles of M2-like Mø, activated Mø phenotypes extend far beyond the simplistic M1 and M2 paradigm, making it challenging to compare Mø phenotypes and functions in differing experimental settings, even within the kidney. In conclusion, our findings show IL-34 increases intrarenal Mø but does not skew the Mø phenotype (within the context of the M1 and M2 markers we explored) during AKI and subsequent CKD.

We wish to highlight the finding that IL-34 and IL-34 receptors are upregulated in ischemia-incited human inflamed kidneys. As IL-34 and IL-34–receptor expression in mouse and human kidneys are similarly upregulated, we speculate that IL-34 in transplanted kidneys may mediate rejection and other forms of renal injury. In conclusion, our mouse experimental data and human data suggest that targeting IL-34 in the kidney and circulation is likely a potential therapeutic strategy to suppress AKI and subsequent CKD.

Methods

Mice. We purchased C57Bl/6 (B6) mice from The Jackson Laboratory and Harlan. Transgenic Tg*(Fms-EGFP)* mice that express eGFP under the control of *Fms* promoter and first intron (MacGreen), were provided by D. Hume (Roslin Institute, University of Edinburgh, Edinburgh, United Kingdom). We backcrossed MacGreen mice onto the B6 background (MacGreen;B6) (4, 23). To generate IL-34 null LacZ$^+$ (*Il34*$^{-/-}$;B6) mice, B6 mice were deleted of *Il34* exons 3–5 and intercrossed with *Il34*$^{LacZ/+}$ offspring, as previously described (18). Transgenic mice expressing *lacZ* under the control of *Csf1* promoter and the first intron (TgN9[*Csf1-Z*]*Ers7*/+) (58) were provided by E.R. Stanley (Albert Einstein College of Medicine, New York, New York, USA) and backcrossed to B6 in our facility at Harvard Medical School, Boston, Massachusetts, USA. IL-34 is required for the development of Langerhans cells (18); thus, in addition to using PCR to detect the deletion of *Il34*, we probed for the loss of Langerhans cells in the epidermis of the ear (59). All breeding housing and colony housing was done at Harvard Medical School.

I/R. We anesthetized female mice (6 weeks of age) and exposed the left kidney through a flank incision. We induced ischemia by clamping the renal pedicle with nontraumatic microaneurysm clamps (Roboz Surgical Instrument Co.). Clamps were removed after 45 minutes. Body temperature was controlled at 36.8°C–37.2°C throughout the procedure.

In situ hybridization. The digoxigenin-labeled (DIG-labeled) antisense oligonucleotide probe for mouse IL-34 was synthesized by in vitro transcription using T7 RNA polymerase and Dig Labeling Mix (Roche Applied Science) from cDNA template amplified from plasmid IL-34–pBS-SK (a gift from E.R. Stanley), and purified with Micro Bio-

Spin 30 Columns (Bio-Rad). Kidneys were fixed in 4% paraformaldehyde overnight, immersed in 30% sucrose/PBS overnight at 4°C, and then embedded and cryostat-sectioned at 20 μm. The kidney sections were prepared and processed for in situ hybridization, as previously described (60). After development, slides were fixed in 4% PFA overnight and dried, and cover slips were mounted for imaging.

β-Galactosidase. β-Galactosidase staining was performed, as previously described (61). Kidneys were fixed in 4% paraformaldehyde for 3 hours at 4°C, embedded and sectioned at 20-μm thick sections. Cryosections were stained with X-gal (catalog X4281C10; Gold Biotechnology) overnight at 37°C and subsequently counterstained with Nuclear Fast Red (catalog N3020; Sigma-Aldrich).

Immunoblotting. Kidney tissues were homogenized in RIPA buffer, and 25 μg total protein was used for immunoblotting, as previously described (62). Blots were probed with mouse monoclonal PTP-ζ Ab (3F8; Developmental Studies Hybridoma Bank, University of Iowa, Iowa City, Iowa, USA). Mouse monoclonal anti-GAPDH Ab (catalog D16H11; Cell Signaling Technology) was used as loading control. Images were captured using ChemiDoc MP imaging system (Bio-Rad).

Immunoprecipitation. We performed immunoprecipitation, as previously described (62). Briefly, kidney tissues were homogenized in CHAPS buffer (30 mM Tris-Cl pH 7.5, 150 mM NaCl, 1% CHAPS containing protease and phosphatase inhibitor cocktails [Sigma-Aldrich]) and 250 μg total protein incubated with 1 μg of PTP-ζ Ab overnight at 4°C. Proteins were transferred onto nitrocellulose membrane, and immunoblotting was performed with polyclonal anti-sheep IL-34 Ab against Asn21-Pro242 (catalog AF5265; R&D Systems). Mouse monoclonal anti-GAPDH, (catalog D16H11; Cell Signaling Technology) and mouse heavy chain IgG were used as loading control for input and immunoprecipitation, respectively.

Renal histopathology. Kidneys were fixed in 10% neutral buffered formalin, embedded in paraffin, sectioned (4 μm), and stained with periodic acid-Schiff (PAS). We scored kidney pathology, as previously detailed (63).

Immunostaining. We stained cryostat-cut mouse kidney sections for the presence of: Mø, using anti–mouse F4/80 Ab (clone BM-8; Invitrogen) and anti–mouse CD68 Ab (clone FA-11; AbD Serotec), as previously detailed (4); proximal tubules using fluorescein isothiocyanate–conjugated (FITC-conjugated) lotus tetragonolobus lectin (LTL; Vector Laboratories) and collecting ducts using biotinylated dolichos biflorus agglutinin (DBA; Vector Laboratories) in combination with Texas red streptavidin (Vector Laboratories); and neutrophils, using anti–mouse Ly6G Ab (clone 1A8, BioLegend). To determine the number of proliferating Mø, cryosections were stained with anti–mouse F4/80 Ab (clone BM-8, Invitrogen), and anti–mouse Ki-67 Ab (clone SP6, Vector Laboratories), followed by FITC-conjugated goat anti-rat IgG Ab (Invitrogen) and Cy3-conjugated goat anti-rabbit IgG Ab (Invitrogen). We enumerated the number of $F4/80^+$/$Ki\text{-}67^+$ cells in 20 high-power fields (HPF).

Kidney biopsy sections were incubated with a primary Ab, rabbit anti–human IL-34 Ab (clone C-19, catalog sc-243072, Santa Cruz Biotechnology Inc.) rabbit anti–human PTP-ζ (catalog ab126497, Abcam), rabbit anti–human CSF-1R (clone C-20, catalog sc-692, Santa Cruz Biotechnology Inc.), rat anti–human Ly6G (clone RB6-8C5, catalog ab25377, Abcam), and mouse anti–human CD68 (clone SPM130, sc-52998, Santa Cruz Biotechnology Inc.). The primary Ab was detected by incubating with biotinylated goat anti-rabbit Ab, rabbit anti-rat, and goat anti-mouse Ab, followed by development with 3-3-diaminobenzidine (Vector Laboratories), as previously detailed (4). Nonspecific binding was determined using rabbit anti-human IgG (IL-34 staining) or rat anti-human (Ly6G staining), or with mouse anti-human IgG (CD68 staining) (eBioscience). We determined the percent-positive TECs or positive infiltrating cells in 10 randomly selected HPFs.

Albuminuria. To quantify albuminuria levels, we analyzed 20 μl urine collected over 8 hours by SDS-PAGE, as previously described (64).

Collagen detection. We stained paraffin sections after rehydration in Picrosirius red solution for 1 hour and rinsed with acidified water. After kidney sections were dehydrated and mounted, the magnitude of staining was analyzed as previously detailed (4) using a Nikon Eclipse E1000 upright fluorescence microscope and Adobe Photoshop CS2.

KIM-1 and NGAL expression. Kidney cryostat-cut sections were stained with polyclonal anti–KIM-1 Ab to determine tubular injury, as previously detailed (4). The NGAL protein was detected using a Luminex xMAP technology, as previously described (65).

Generating BMMø. Mø were generated from mouse BM, as previously detailed (3).

Stimulating Mø using hypoxic TEC supernatant. We isolated and expanded TECs from *Il34*$^{-/-}$ and WT kidneys, as previously reported (3). We cultured TECs for 24 hours under hypoxic conditions with 99% N_2/1% O_2 at 37°C in a hypoxic chamber and evaluated viability using both microscopic analysis of trypan blue exclusion staining and flow cytometry analysis of PI staining. Cell supernatant was collected after hypoxia and was used to stimulate BMMø. To derive BMMø, we cultured BM in L929 conditioned media and then starved BMMø in serum-free DMEM medium without L929 for 2 hours. We incubated BMMø with supernatant from hypoxic *Il34*$^{-/-}$ and WT TECs. To restore IL-34 in *Il34*$^{-/-}$ TEC supernatants, we added rIL-34 protein to hypoxic *Il34*$^{-/-}$ TEC supernatant at concentrations ranging from 50–500 ng/mL. To block IL-34 and CSF-1, anti–IL-34 Ab (10 μg/ml, catalog AF5195, R&D Systems) and anti–CSF-1 Abs (2 μg/ml, 552513, BD Biosciences) neutralizing Abs were added to hypoxic WT and *Il34*$^{-/-}$ TEC supernatants during incubation with BMMø. After incubating for 24 hours, we analyzed Mø proliferation with the MTT assay (Roche Diagnostics) and BrdU incorporation (10 μM, 2 hours) using flow cytometry.

ELISA. To quantify IL-34 and CSF-1 levels, in the kidney, circulation and hypoxic and normoxic TEC supernatants, samples were analyzed using a mouse IL-34 ELISA (R&D Systems) according to the manufacturer's instructions and a mouse CSF-1 ELISA (7). We measured human IL-34 levels with a human IL-34 ELISA (R&D Systems) according to the manufacturer's instructions. All measurements were made in duplicate.

qPCR. qPCR was performed, as previously described (4). We detected *Csf1*, *Il34*, *Fms*, *Ptprz1* and *Gapdh* using QuantiTect Primer Assays (QIAGEN) or using primers purchased from Invitrogen and Integrated DNA Technologies: *Csf1,* forward 5′-GGCTTGGCTTGGGATGATTCT-3′, reverse 5′-GAGGGTCTGGCAGGTACTC-3′; *Il34*, forward 5′-TTGCTGTAAACAAAGCCCCAT-3′, reverse 5′-CCGAGACAAAGGGTACACATTT-3′; *Fms*, forward 5′-TGTCATCGAGCCTAGTGGC-3′, reverse 5′-CGGGAgATTCAGGGTCCAAg-3′; and *Gapdh*, forward 5′-AGGTCGGTGTGAACGGATTTG-3′, reverse 5′-TGTAGACCATGTAGTTGAGGTCA-3′. Other purchased primers used in this study were: collagen I, forward 5′-TgACTGGAAGAGCGGAGAGT-3′, reverse 5′-GTTCGGCTGATGTACCAgT-3′; fractalkine/*Cx3cl1*, forward 5′-TCGGACTTTGTTGGTTCCTC-3′, reverse 5′-CAAAATGG-

CACAGACATTGG-3′; *Kim1*, forward 5′-TAAACCAGAGATTCCCA-CAC-3′, reverse 5′-GATCTTGTTGAAATAGTCGTG-3′; *Mcp-1/Ccl2*, forward 5′-GCTTGAGGTGGTTGTGGAAAA-3′, reverse 5′-CTCACCT-gCTgCTACTCATTC-3′; *Mip1a/Ccl3*, forward 5′-TCTCCACCACT-GCCCTTgCT-3′, reverse 5′-GGCGTGGAATCTTCCGGCTGT-3′; and *Ptprz1*, forward 5′-GGAGTATCCAACAGTTCAGAGGC-3′, reverse 5′-AAGTCAGGGCAGACACGATCAC-3′. *Ip10/Cxcl10* expression was examined using primers designed by Applied Biosystems. The data were analyzed by the ΔΔ-CT method.

Flow cytometry. We prepared and stained single-cell suspensions from kidneys, RBC-lysed BM, and blood cells for intracellular and extracellular antigens as previously described (63).

Antibodies for flow cytometry. We used the following antibodies from BioLegend for FACS analysis: FITC-conjugated anti–mouse/human CD11b Ab (clone M1/70); phycoerythrin-conjugated (PE-conjugated) anti–mouse CD115 Ab (clone AFS98); FITC-conjugated anti–mouse CD206 Ab (clone 15-2); PE-conjugated anti–mouse Ly6C Ab (clone HK1.4); PE-conjugated anti–Dectin-1 Ab (clone RH1); PerCP/Cy5.5-conjugated anti–mouse/human CD11b Ab (clone M1/70); allophycocyanin-conjugated (APC-conjugated) anti–mouse F4/80 Ab (clone BM-8); pacific blue–conjugated anti–mouse CD45 Ab (clone 30-F11); APC/Cy7-conjugated anti–mouse Ly6G Ab (clone 1A8); biotinylated anti–mouse Ly6C Ab (clone HK1.4); FITC-conjugated TNFα (clone MP6-XT22); and FITC-conjugated streptavidin. In addition, we used FITC-conjugated anti–CD3ε (clone 145-2C11) Ab from eBioscience, FITC-conjugated anti–iNOS-2 (6/iNOS/NOS Type II) Ab from BD Biosciences, and PE-conjugated anti–Arginase-1 polyclonal Ab from R&D Systems.

BrdU incorporation assay. We injected mice (i.p.) with BrdU (2 mg/mouse, Sigma-Aldrich) 3 hours before sacrifice. $BrdU^+$ cells were analyzed with an anti-BrdU Ab (clone Bu20a, BioLegend) by flow cytometry.

Adoptive transfer. We isolated BM from MacGreen;B6 mice and adoptively transferred the $eGFP^+$ cells (2×10^7 and 1×10^7) by injection into the tail vein of *Il34*$^{-/-}$ and WT mice 24 hours after I/R. Mice were sacrificed 3 hours later. Kidney and blood samples were processed to detect $eGFP^+$ cells using flow cytometry, as previously detailed (63).

Recruitment assays. BM (2×10^7) cells from MacGreen mice ($eGFP^+$ myeloid cells) were stimulated either with active or heat-inactivated (95°C, 30 minutes) PTx, as previously described (66), and adoptively transferred into WT B6 mice after I/R (d1). After 3 hours, kidneys and blood were collected and analyzed by flow cytometry. The viability of donor cells was tested using PI (Sigma-Aldrich) and analyzed by flow cytometry.

Chemotaxis assay. TECs isolated from B6 mice were incubated with TNFα (25 ng/ml) with and without anti–IL-34 Ab (catalog AF5195, R&D Systems) and anti–MCP-1 Ab (catalog 479-JE-010, R&D Systems) using increasing concentrations (1.25–40 μg/ml). Following stimulation for 24 hours, the supernatant was replaced and stimulated TECs were coincubated with primary isolated Mø from B6 mice using a 2-chamber, 96-well plate separated by a polycarbonate membrane (pore size: 5 μg/ml). To quantify Mø chemotaxis, samples were analyzed in duplicate according to the manufacturer's instructions (Cell Biolabs Inc.).

Serum and renal biopsy specimens. The demographic and clinical characteristics for the cohort used in this study are listed in Supplemental Table 1, A and B. Human kidney sections from transplanted kidney biopsies and donor biopsies prior to transplantation were provided by the Department of Pathology, Friedrich-Alexander University of Erlangen-Nuernberg, Erlangen, Germany. Donor-kidney biopsies from living and deceased donors were evaluated before and after reperfusion. The following criteria were used to define these patient biopsies: living donors were defined as healthy individuals donating their kidney to a family member; deceased donors were defined as patients who have complete and irreversible loss of brain function; "before reperfusion" was defined as a biopsy after removing the kidney from the donor prior to transplantation; and "after reperfusion" was defined as a biopsy after kidney transplantation into the recipient. Renal pathologists, without access to the patient's clinical data, evaluated these biopsies according to the BANFF renal allograft pathology classification (67–69). We analyzed serum samples from patients with histology-proven diagnosis of cellular rejection or engraftment (no rejection). Blood samples were collected, centrifuged, aliquoted, and stored at –30°C prior to analysis.

Statistics. Data represent the mean ± SEM prepared using GraphPad Prism software, version 5.0. We used the nonparametric Mann–Whitney *U* test to evaluate *P* values.

Study approval. Use of mice in this study was reviewed and approved by the Standing Committee on Animals in the Harvard Medical School, in adherence to standards set in the *Guide for the Care and Use of Laboratory Animals* (8th edition, The National Academies Press, revised 2011). Specimens for human study analysis were taken from patients after informed consent. The use of these specimens was approved by the Standing Committee for Clinical Studies of the Johannes-Gutenberg University, Mainz, Germany, in adherence to the Declaration of Helsinki and analyzed retrospectively.

Acknowledgments

We wish to acknowledge the Alliance for Lupus Research (V.R. Kelley) and the MAIFOR research program of the Johannes-Gutenberg University Mainz and the Deutsche Forschungsgemeinschaft (J. Weinmann-Menke; ME3194/2-1) for supporting this study. J.-H. Baek was supported by Deutsche Forschungsgemeinschaft Fellowship (BA 4875/1-1) and R. Zeng was partially supported by National Nature Science Foundation of China (81270771). We wish to thank Filisia Agus, Kirsten Marija Levandowski, Sabbisetti S. Venkata, and Wing-Ki Cheng for technical assistance, and Benjamin Humphreys for conceptual discussions.

Address correspondence to: Vicki Rubin Kelley, Harvard Institute of Medicine, 4 Blackfan Circle, Boston, Massachusetts 02115, USA. Phone: 617.525.5915; E-mail: vkelley@rics.bwh.harvard.edu.

Rui Zeng's current affiliation is: Division of Nephrology, Tongji Hospital, Huazhong University of Science and Technology, Wuhan, China.

1. Lee S, et al. Distinct macrophage phenotypes contribute to kidney injury and repair. *J Am Soc Nephrol*. 2011;22(2):317–326.
2. Lech M, et al. Macrophage phenotype controls long-term AKI outcomes--kidney regeneration versus atrophy. *J Am Soc Nephrol*. 2014;25(2):292–304.
3. Iwata Y, et al. Aberrant macrophages mediate defective kidney repair that triggers nephritis in lupus-susceptible mice. *J Immunol*. 2012;188(9):4568–4580.
4. Menke J, et al. CSF-1 signals directly to renal tubular epithelial cells to mediate repair in mice.

J Clin Invest. 2009;119(8):2330–2342.
5. Bloom RD, Florquin S, Singer GG, Brennan DC, Kelley VR. Colony stimulating factor-1 in the induction of lupus nephritis. *Kidney Int*. 1993;43(5):1000–1009.
6. Lenda DM, Stanley ER, Kelley VR. Negative role of colony-stimulating factor-1 in macrophage, T cell, and B cell mediated autoimmune disease in MRL-Fas(lpr) mice. *J Immunol*. 2004;173(7):4744–4754.
7. Menke J, et al. Circulating CSF-1 promotes monocyte and macrophage phenotypes that enhance lupus nephritis. *J Am Soc Nephrol*. 2009;20(12):2581–2592.
8. Menke J, Iwata Y, Rabacal WA, Basu R, Stanley ER, Kelley VR. Distinct roles of CSF-1 isoforms in lupus nephritis. *J Am Soc Nephrol*. 2011;22(10):1821–1833.
9. Guilbert LJ, Stanley ER. Specific interaction of murine colony-stimulating factor with mononuclear phagocytic cells. *J Cell Biol*. 1980;85(1):153–159.
10. Sherr CJ, Rettenmier CW, Sacca R, Roussel MF, Look AT, Stanley ER. The c-fms proto-oncogene product is related to the receptor for the mononuclear phagocyte growth factor, CSF-1. *Cell*. 1985;41(3):665–676.
11. Tushinski RJ, Oliver IT, Guilbert LJ, Tynan PW, Warner JR, Stanley ER. Survival of mononuclear phagocytes depends on a lineage-specific growth factor that the differentiated cells selectively destroy. *Cell*. 1982;28(1):71–81.
12. Byrne PV, Guilbert LJ, Stanley ER. Distribution of cells bearing receptors for a colony-stimulating factor (CSF-1) in murine tissues. *J Cell Biol*. 1981;91(3):848–853.
13. Wiktor-Jedrzejczak W, et al. Total absence of colony-stimulating factor 1 in the macrophage-deficient osteopetrotic (op/op) mouse. *Proc Natl Acad Sci U S A*. 1990;87(12):4828–4832.
14. Dai XM, et al. Targeted disruption of the mouse colony-stimulating factor 1 receptor gene results in osteopetrosis, mononuclear phagocyte deficiency, increased primitive progenitor cell frequencies, and reproductive defects. *Blood*. 2002;99(1):111–120.
15. Wei S, et al. Functional overlap but differential expression of CSF-1 and IL-34 in their CSF-1 receptor-mediated regulation of myeloid cells. *J Leukoc Biol*. 2010;88(3):495–505.
16. Lin H, et al. Discovery of a cytokine and its receptor by functional screening of the extracellular proteome. *Science*. 2008;320(5877):807–811.
17. Chihara T, et al. IL-34 and M-CSF share the receptor Fms but are not identical in biological activity and signal activation. *Cell Death Differ*. 2010;17(12):1917–1927.
18. Wang Y, et al. IL-34 is a tissue-restricted ligand of CSF1R required for the development of Langerhans cells and microglia. *Nat Immunol*. 2012;13(8):753–760.
19. Nandi S, et al. Receptor-type protein-tyrosine phosphatase zeta is a functional receptor for interleukin-34. *J Biol Chem*. 2013;288(30):21972–21986.
20. Rubin Kelley V, Bloom RD, Yui MA, Martin C, Price D. Pivotal role of colony stimulating factor-1 in lupus nephritis. *Kidney Int Suppl*. 1994;45:S83–85.
21. Menke J, et al. Sunlight triggers cutaneous lupus through a CSF-1-dependent mechanism in MRL-Fas(lpr) mice. *J Immunol*. 2008;181(10):7367–7379.
22. Lenda DM, Kikawada E, Stanley ER, Kelley VR. Reduced macrophage recruitment, proliferation, and activation in colony-stimulating factor-1-deficient mice results in decreased tubular apoptosis during renal inflammation. *J Immunol*. 2003;170(6):3254–3262.
23. Jang MH, et al. Distinct in vivo roles of colony-stimulating factor-1 isoforms in renal inflammation. *J Immunol*. 2006;177(6):4055–4063.
24. Alikhan MA, et al. Colony-stimulating factor-1 promotes kidney growth and repair via alteration of macrophage responses. *Am J Pathol*. 2011;179(3):1243–1256.
25. Zhang MZ, et al. CSF-1 signaling mediates recovery from acute kidney injury. *J Clin Invest*. 2012;122(12):4519–4532.
26. Bonventre JV, Yang L. Cellular pathophysiology of ischemic acute kidney injury. *J Clin Invest*. 2011;121(11):4210–4221.
27. Bolignano D, et al. Neutrophil gelatinase-associated lipocalin (NGAL) and progression of chronic kidney disease. *Clin J Am Soc Nephrol*. 2009;4(2):337–344.
28. Hashimoto D, et al. Tissue-resident macrophages self-maintain locally throughout adult life with minimal contribution from circulating monocytes. *Immunity*. 2013;38(4):792–804.
29. Greter M, et al. Stroma-derived interleukin-34 controls the development and maintenance of langerhans cells and the maintenance of microglia. *Immunity*. 2012;37(6):1050–1060.
30. Mantovani A, Sozzani S, Locati M, Allavena P, Sica A. Macrophage polarization: tumor-associated macrophages as a paradigm for polarized M2 mononuclear phagocytes. *Trends Immunol*. 2002;23(11):549–555.
31. Martinez FO, Sica A, Mantovani A, Locati M. Macrophage activation and polarization. *Front Biosci*. 2008;13:453–461.
32. Murray PJ, Wynn TA. Protective and pathogenic functions of macrophage subsets. *Nat Rev Immunol*. 2011;11(11):723–737.
33. Terasaki PI, Cecka JM, Gjertson DW, Takemoto S. High survival rates of kidney transplants from spousal and living unrelated donors. *N Engl J Med*. 1995;333(6):333–336.
34. Solary E, Droin N. The emerging specificities of interleukin-34. *J Leukoc Biol*. 2014;95(1):3–5.
35. Nakamichi Y, Udagawa N, Takahashi N. IL-34 and CSF-1: similarities and differences. *J Bone Miner Metab*. 2013;31(5):486–495.
36. Zelante T, Ricciardi-Castagnoli P. The yin-yang nature of CSF1R-binding cytokines. *Nat Immunol*. 2012;13(8):717–719.
37. Masteller EL, Wong BR. Targeting IL-34 in chronic inflammation. *Drug Discov Today*. 2014;19(8):1212–1216.
38. Dai XM, Zong XH, Sylvestre V, Stanley ER. Incomplete restoration of colony-stimulating factor 1 (CSF-1) function in CSF-1-deficient Csf1op/Csf1op mice by transgenic expression of cell surface CSF-1. *Blood*. 2004;103(3):1114–1123.
39. Preisser L, et al. IL-34 and macrophage colony-stimulating factor are overexpressed in hepatitis C virus fibrosis and induce profibrotic macrophages that promote collagen synthesis by hepatic stellate cells. *Hepatology*. 2014;60(6):1879–1890.
40. Peles E, Schlessinger J, Grumet M. Multi-ligand interactions with receptor-like protein tyrosine phosphatase beta: implications for intercellular signaling. *Trends Biochem Sci*. 1998;23(4):121–124.
41. Li YS, et al. Cloning and expression of a developmentally regulated protein that induces mitogenic and neurite outgrowth activity. *Science*. 1990;250(4988):1690–1694.
42. Peles E, et al. The carbonic anhydrase domain of receptor tyrosine phosphatase beta is a functional ligand for the axonal cell recognition molecule contactin. *Cell*. 1995;82(2):251–260.
43. Milev P, et al. High affinity binding and overlapping localization of neurocan and phosphacan/protein-tyrosine phosphatase-zeta/beta with tenascin-R, amphoterin, and the heparin-binding growth-associated molecule. *J Biol Chem*. 1998;273(12):6998–7005.
44. Bethunaickan R, Berthier CC, Zhang W, Kretzler M, Davidson A. Comparative transcriptional profiling of 3 murine models of SLE nephritis reveals both unique and shared regulatory networks. *PLoS One*. 2013;8(10):e77489.
45. Zeng F, Singh AB, Harris RC. The role of the EGF family of ligands and receptors in renal development, physiology and pathophysiology. *Exp Cell Res*. 2009;315(4):602–610.
46. Tang J, Liu N, Zhuang S. Role of epidermal growth factor receptor in acute and chronic kidney injury. *Kidney Int*. 2013;83(5):804–810.
47. Tesch GH, Schwarting A, Kinoshita K, Lan HY, Rollins BJ, Kelley VR. Monocyte chemoattractant protein-1 promotes macrophage-mediated tubular injury, but not glomerular injury, in nephrotoxic serum nephritis. *J Clin Invest*. 1999;103(1):73–80.
48. Summers C, Rankin SM, Condliffe AM, Singh N, Peters AM, Chilvers ER. Neutrophil kinetics in health and disease. *Trends Immunol*. 2010;31(8):318–324.
49. Foucher ED, et al. IL-34 induces the differentiation of human monocytes into immunosuppressive macrophages. Antagonistic effects of GM-CSF and IFNgamma. *PLoS One*. 2013;8(2):e56045.
50. Swenson-Fields KI, et al. Macrophages promote polycystic kidney disease progression. *Kidney Int*. 2013;83(5):855–864.
51. Toki D, et al. The role of macrophages in the development of human renal allograft fibrosis in the first year after transplantation. *Am J Transplant*. 2014;14(9):2126–2136.
52. Ikezumi Y, et al. Alternatively activated macrophages in the pathogenesis of chronic kidney allograft injury. *Pediatr Nephrol*. 2015;30(6):1007–1017.
53. Anders HJ, Ryu M. Renal microenvironments and macrophage phenotypes determine progression or resolution of renal inflammation and fibrosis. *Kidney Int*. 2011;80(9):915–925.
54. Pellicoro A, Ramachandran P, Iredale JP, Fallowfield JA. Liver fibrosis and repair: immune regulation of wound healing in a solid organ. *Nat Rev Immunol*. 2014;14(3):181–194.
55. Li D, et al. IL-33 promotes ST2-dependent lung fibrosis by the induction of alternatively activated macrophages and innate lym-

phoid cells in mice. *J Allergy Clin Immunol*. 2014;134(6):1422–1432 e1411.
56. Gratchev A, et al. Alternatively activated macrophages differentially express fibronectin and its splice variants and the extracellular matrix protein betaIG-H3. *Scand J Immunol*. 2001;53(4):386–392.
57. Willment JA, et al. Dectin-1 expression and function are enhanced on alternatively activated and GM-CSF-treated macrophages and are negatively regulated by IL-10, dexamethasone, and lipopolysaccharide. *J Immunol*. 2003;171(9):4569–4573.
58. Ryan GR, et al. Rescue of the colony-stimulating factor 1 (CSF-1)-nullizygous mouse (Csf1(op)/Csf1(op)) phenotype with a CSF-1 transgene and identification of sites of local CSF-1 synthesis. *Blood*. 2001;98(1):74–84.
59. Baek JH, Birchmeier C, Zenke M, Hieronymus T. The HGF receptor/Met tyrosine kinase is a key regulator of dendritic cell migration in skin immunity. *J Immunol*. 2012;189(4):1699–1707.
60. Yu J, et al. Identification of molecular compartments and genetic circuitry in the developing mammalian kidney. *Development*. 2012;139(10):1863–1873.
61. Kobayashi A, et al. Six2 defines and regulates a multipotent self-renewing nephron progenitor population throughout mammalian kidney development. *Cell Stem Cell*. 2008;3(2):169–181.
62. Ajay AK, Kim TM, Ramirez-Gonzalez V, Park PJ, Frank DA, Vaidya VS. A bioinformatics approach identifies signal transducer and activator of transcription-3 and checkpoint kinase 1 as upstream regulators of kidney injury molecule-1 after kidney injury. *J Am Soc Nephrol*. 2014;25(1):105–118.
63. Menke J, et al. Programmed death 1 ligand (PD-L) 1 and PD-L2 limit autoimmune kidney disease: distinct roles. *J Immunol*. 2007;179(11):7466–7477.
64. Schaldecker T, et al. Inhibition of the TRPC5 ion channel protects the kidney filter. *J Clin Invest*. 2013;123(12):5298–5309.
65. Vaidya VS, et al. Regression of microalbuminuria in type 1 diabetes is associated with lower levels of urinary tubular injury biomarkers, kidney injury molecule-1, and N-acetyl-beta-D-glucosaminidase. *Kidney Int*. 2011;79(4):464–470.
66. Masuyama J, et al. Characterization of the 4C8 antigen involved in transendothelial migration of CD26(hi) T cells after tight adhesion to human umbilical vein endothelial cell monolayers. *J Exp Med*. 1999;189(6):979–990.
67. Solez K, et al. Banff 07 classification of renal allograft pathology: updates and future directions. *Am J Transplant*. 2008;8(4):753–760.
68. Mengel M, et al. Banff 2011 Meeting report: new concepts in antibody-mediated rejection. *Am J Transplant*. 2012;12(3):563–570.
69. Haas M, et al. Banff 2013 meeting report: inclusion of c4d-negative antibody-mediated rejection and antibody-associated arterial lesions. *Am J Transplant*. 2014;14(2):272–283.